Modeling Geomagnetically Induced Currents on Networked Conductors

by

Peter F. Mayer

A Thesis submitted to the Faculty of Graduate Studies of

The University of Manitoba

in partial fulfillment of the requirements of the degree of

MASTER OF SCIENCE

Department of Electrical and Computer Engineering

The University of Manitoba

Winnipeg

Canada

Copyright © 2005 by Peter Mayer

THE UNIVERSITY OF MANITOBA

FACULTY OF GRADUATE STUDIES
*****
COPYRIGHT PERMISSION

Modeling Geomagnetically Induced Currents on Networked Conductors

by

Peter F. Mayer

A Thesis/Practicum submitted to the Faculty of Graduate Studies of The University of Manitoba in partial fulfillment of the requirement of the degree

of

Master of Science

Peter F. Mayer © 2006

Permission has been granted to the Library of the University of Manitoba to lend or sell copies of this thesis/practicum, to the National Library of Canada to microfilm this thesis and to lend or sell copies of the film, and to University Microfilms Inc. to publish an abstract of this thesis/practicum.

This reproduction or copy of this thesis has been made available by authority of the copyright owner solely for the purpose of private study and research, and may only be reproduced and copied as permitted by copyright laws or with express written authorization from the copyright owner.

Acknowledgements

My former supervisor Dr. David R. Swatek made this project possible, and for that I am deeply grateful.

I am indebted to my supervisor, Brett Davies, and my employer, Manitoba Hydro, whose helpful encouragement and generous support allowed this work's completion.

Finally, I would like to thank my advisor, Dr. Udaya Annakkage. His guidance, patience and efforts on my behalf made this Thesis possible, and are greatly appreciated.

Abstract

The modeling of Geomagnetically Induced Currents (GICs) on networked conductors is discussed. A non-uniform influence near the surface of the Earth is modeled. A complex-image calculation method that models the auroral electrojet as an infinite current filament is used. Theoretical examples show the necessity of using in-line voltage sources for modeling the effects of non-uniform fields. A method for calculating the total voltage induced along the path of an arbitrary conductor is described. A power system simulator, PSCAD, is used to compare currents in networks where induction is represented by grounded and in-line voltage sources. The results show that in-line voltage sources are required to correctly model realistic GIC flow in networks.

Contents

List of Figures

List of Tables

Nomenclature

ang	angle of electrojet from true North [deg]
AU	Astronomical Unit, approximately equal to the average distance between the Earth and the Sun
Bz	magnetic flux density in the z direction [T]
c	the hypotenuse of a right-triangle
CME	Coronal Mass Ejection
cx	UTM x-coordinate directly under electrojet
cy	UTM y-coordinate directly under electrojet
d	distance between point along conductor and point directly under electrojet [m]
D	distance between points on the surface of the Earth [m]
E	electric field magnitude [V/m]
f	electrojet frequency [Hz]
GIC	Geomagnetically Induced Current
h	electrojet height [m]
h_n	height of the n^{th} soil layer [m]
I	electrojet current [A]
j	complex variable ($\sqrt{-1}$)
k_n	wave number of the n^{th} layer
m	slope of a line
north	logical input data northern or southern ground model
p	complex depth [m]

R	reflection coefficient
R_e	radius of the Earth [m]
RMS	Root Mean Squared
UTM	Universal Transverse Mercator
V	RMS voltage applied to transmission line [V]
V_{AB}	induced voltage on a conductor between points A and B [V]
V_l	voltage induce along the length of a conductor [V]
V_{seg}	voltage induced on conductor segment [V]
V_{ss}	voltage induced on conductor sub-segment [V]
x	x coordinate
y	y coordinate
Z	surface impedance [Ω]
γ	angle from East-West axis [deg]
Γ_n	reflection coefficient of the n^{th} layer
Δx	x distance in conductor sub-section [m]
Δy	y distance in conductor sub-section [m]
ε_n	permittivity of the n^{th} layer [F/m]
λ	constant of integration
μ_0	permeability of free space [H/m]
μ_n	permeability of the n^{th} layer [M/m]
ρ_n	ground resistivity of the n^{th} layer [Ω m]
σ_n	conductivity at the nth layer [S/m]
ω	angular frequency [rad./s.]

Chapter 1

Introduction

1.1 Geomagnetically Induced Currents (GICs)

Geomagnetically Induced Currents (GICs) are the undesirable result of changes in or motion of the auroral electrojet, a large current that flows in the upper atmosphere near the Earth's poles. The auroral electrojet is a consequence of perturbations in the Earth's magnetic field caused by changes in the solar wind. Geomagnetically Induced Currents occur on long conductors such as power lines, communication cables and pipelines. The length of these conductors allows significant induction from the auroral electrojet and their relatively low resistance allows currents to flow along them. The resulting quasi-dc currents that flow in power transmission lines and transformers are of particular interest, as they cause heating and half-wave saturation when they flow through transformer neutral windings. The heating can shorten transformer life and the saturation leads to increased reactive power consumption (Tay, Swift, 1985). This increase in reactive power consumption can cause protection misoperation and even system-wide voltage collapse (Kappenman, Albertson, 1990).

1.2 Modeling GICs in Networks

Because transmission lines are almost always part of a large electrical network, the behaviour of GIC in a given transmission line or transformer is strongly influenced by the

entire network (Boteler, 1994). It is therefore desirable to model as much of the electrical network as possible. Because the electric field is strongest directly under the auroral electrojet and weakens with distance, the amount of induction each transmission line in a transmission system will experience is variable. This is especially true if the transmission system covers a large geographic area or is located near the poles. The auroral electrojets flow near the poles and the amount of induction is most variable close to them (Pirjola, Viljanen, 1989). For many years Earth surface potentials have been used to explain the occurrence of GICs (Albertson, Thorson, Miske, 1974, EPRI, 2002). In fact, the surface potentials between stations do not drive GICs, but share a common cause: Induction from the auroral electrojet. Modeling GICs as a result of potential differences between station grounds is not only conceptually reversed, but it makes it impossible to model the results of realistic, non-uniform induction on a network (Boteler, Prijola, 1998b). Modeling the induction along the transmission lines with voltage sources in series with the transmission lines enables accurate network representations of networks under non-uniform fields and more closely resembles the physical phenomenon causing the GIC.

1.3 Motivation

In the operation of electric power systems, predictions of GIC magnitudes in transformer neutral windings can be used in writing specifications for new equipment, in protection design and in load-flow studies (Manitoba Hydro, 1977; IEEE, 1996). In the past, grounded voltage sources have been incorrectly used to represent a non-uniform field in an electric power network (Albertson, et al., 1981). The GIC that this model predicted at a Manitoba Hydro station was more than double what has actually been observed

(Jayasinghe, McLaren, Goldsborough, 1993). This magnitude of error, whether the value is too high or too low, can lead to incorrect specifications for transformers, sub-optimal distribution of monitoring equipment and misplaced protection measures. More accurate predictions of GIC flow in power networks could be used to focus GIC mitigation measures where they are most needed (Bolduc et al., 2005). Ideally, the more closely a model can simulate the behaviour of the whole power system, including excess harmonics and greater reactive power demand, the better prepared power utilities can be for GICs.

1.4 Scope of Thesis

This thesis describes some of the causes of and influences on the auroral electrojet. It then compares methods of calculating the electric field at the Earth's surface resulting from a given electrojet. A complex-image method is chosen for use in this thesis because of its simplicity and accuracy. Examples are used to show the importance of using in-line voltage sources instead of grounded voltage sources for modeling GIC flow in networks. Geographic information about the path of transmission lines and the electrojet are used together to find how much voltage is induced on a given transmission line. A power system simulator, PSCAD, is used to create 2 simple networks to compare the results of in-line and grounded voltage sources. The models are compared under different electrojet orientations and the results confirm the prediction that grounded voltage sources are unable to correctly model the GIC flow.

Chapter 2

The Auroral Electrojet

2.1 Introduction

The Sun is a very dynamic object. One of the effects of this dynamic behaviour on the Earth can be observed in the form of magnetic storms and substorms (Campbell, 1997). These periods of abnormal and variable magnetic readings have been observed for hundreds of years, but it was not until the 1960s that their mechanisms have begun to be explained. When solar disruptions influence the Earth's magnetic field, the geomagnetic field, these field changes can be coupled to transmission lines, communication cables and pipelines near the surface. The complex processes that produce these effects make the precise locations and natures of the disturbances to technological systems nearly impossible to predict. This chapter will describe the causes and mechanisms by which these disturbances are created.

2.2 The Solar Wind

The Sun is constantly ejecting charged particles in all directions (Goldstein, 1998). This "solar wind" is caused by the extremely high temperature of the outermost layer of the Sun, the corona. The temperature in the corona is so high (~1 000 000 K) that gasses form plasma. Plasma is a gas that has been ionized to the point that its behaviour is

influenced by electrical and magnetic forces. The pressure of this coronal plasma is much higher than the pressure in interstellar space, and so it radiates outward.

Plasma can be approximated as being a perfect electrical conductor (Campbell, 1997). When a conductor is moved in a magnetic field a current is induced inside it. The direction of this induced current is such that its magnetic field will oppose the field that created it. This means that any magnetic field present in a body of plasma will not be affected by the magnetic field that it moves through. The excellent electrical conductivity allows the induced current to shield the initial magnetic field of the plasma body from the field it passes through by opposing and cancelling out the background field. This effect allows what is described as the "frozen-in magnetic field" of a plasma body and is important to understanding solar storms.

Because its behaviour is strongly influenced by electromagnetic effects, plasma can only travel along magnetic lines of flux and can only escape the Sun on open magnetic field lines (Goldstein, 1998). These open field lines are more common near the magnetic poles. Because the base of the magnetic field line stays stationary in the sun as it rotates, the magnetic field lines spiral out into space at low latitudes and are twisted near the poles, this effect is shown in figure 2.1. This twisting at high solar latitudes can cause Alfvén waves, which are changes in the direction of the magnetic field in the plasma with no associated change in plasma density or magnetic field strength.

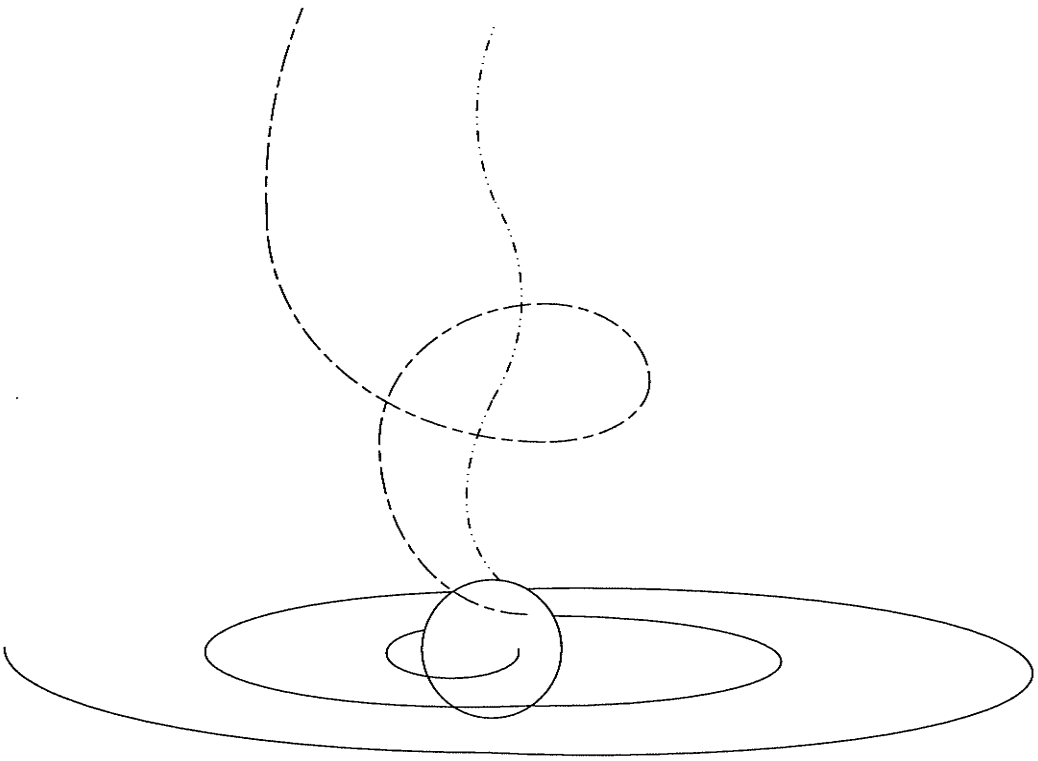

Figure 2.1 Plasma travels away from the Sun on magnetic lines of flux that spiral out near the equator and become twisted near the poles.

Another source of changing magnetic fields in the solar wind is a magnetic cloud (Suess, Tsurutani, 1998). A magnetic cloud is an area of solar wind plasma characterized by a high magnetic field (~25nT, where the ambient field in the solar wind is ~5nT at 1 AU) and a smooth rotation of the magnetic field direction in one plane (Tsurutani, Gonzalez, 1997; Farrugia et al., 1997).

Corotating structures can cause large variations in the magnetic field intensity and direction of the solar wind (Jackson, 1997). These cyclical events result from fixed locations with tortured magnetic fields. As these locations rotate with the Sun, their influences reoccur roughly every 27 days.

Sunspots are an example of a feature that rotates with the Sun's surface (Goldstein, 1998). These locations may provide extra open magnetic field lines where high-speed plasma can flow out. Like the plasma flowing out of the Sun's polar regions, these streams may be subject to Alfvén waves.(Tsurutani, Gonzalez, 1997; Gallant, 1980)

Since plasma can only travel on open magnetic field lines, all plasma is either travelling on a "toward" field line connected to a southern magnetic pole or an "away" field line attached to a Northern magnetic pole (Campbell, 1997). As the sun rotates, the source of the solar wind in a given fixed location may change from a toward to an away field line. As this transition occurs the plasma on either side of the boundary is compressed and disturbed.

For reasons which are not well understood there are occasional explosive ejections of plasma outward from the corona (Tsurutani, Gonzalez, 1997). These Coronal Mass Ejections (CMEs) can travel much faster than the "quiet-time" solar wind, up to 1000km/s vs. <500km/s. If a CME is travelling very fast through inter-planetary space it can push the ambient plasma that was released before the ejection ahead of it in a manner similar to the bow-wave on a ship or the shockwave in front of a supersonic airplane.

Unlike those familiar effects, the particle interaction in the plasma is not caused by collisions but rather electric and magnetic forces. Because of its supersonic shockwave-like behaviour the boundary between the undisturbed solar wind and the fast moving CME is known as the "shock". Figure 2.2 shows a representation of a CME. The ion density across the shock is increased from a normal value of ~5 cm^{-3} to a value roughly 10 times as high as particles are pushed out in front of the CME. Because of this compression of plasma in the shock wave, the magnetic field is also increased several fold across the shock wave. This area of compressed plasma behind the shock is called the "sheath", and behind this is the "driver gas". Sometimes the driver gas ejected from the corona will be a magnetic cloud, and this will cause a rapid change in the direction of the magnetic field.

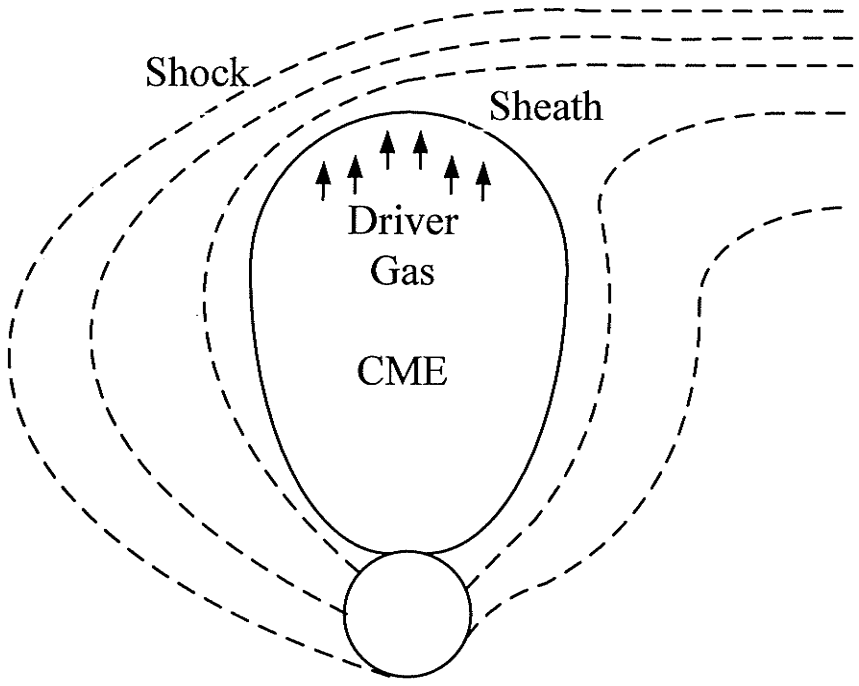

Figure 2.2 **A Coronal Mass Ejection (CME) compresses a shockwave in front of it as it travels through the ambient solar wind.**

The magnetic field of the Sun is extremely complicated. Instead of acting as a rigid body, the Sun's equatorial regions move faster than its poles. This difference twists and distorts the magnetic field lines in the sun (as show in figure 2.3). Because of this distortion, the magnetic field "locked-in" to plasma and ejected from the Sun may be oriented in any direction and will fluctuate with time. The rate and intensity of these fluctuations will depend on the type and strength of phenomena that caused them, where the plasma was ejected and how quickly it is travelling. There are many types of magnetic field transients and phenomena and none are particularly well understood. Those presented above are simplified explanations of some of the more likely causes for geomagnetic disturbances large enough to interfere with technological systems.

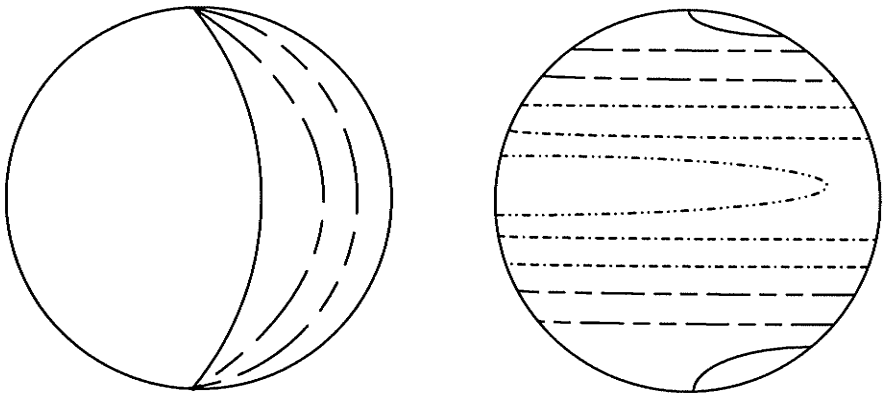

Figure 2.3 Solar magnetic field lines are twisted and distorted by the faster rotating equatorial region.

2.3 The Magnetoshpere and Ionosphere

The ionosphere is an area of the atmosphere populated by weakly ionized plasmas that begins at an altitude of ~60km and extends to ~500km or higher (Richmond, 1996). Above this altitude a distinction is made where the density of neutral particles is low enough that the Earth's magnetic field dominates the behaviour of charged particles. This region is called the magnetosphere. Beyond the magnetosphere the motion of charged particles is dictated by the solar wind and the Sun's magnetic field.

As the densities of different ions rise and fall with increasing altitude in the ionosphere the density of neutral particles steadily decreases (Richmond, 1996). Because of this variability different effects predominate at different levels. Of interest in examining geomagnetic activity is the change in electrical conductivity with altitude. At high ionospheric altitudes the behaviour of charged particles is only weakly influenced by collisions, and so they move almost exclusively along lines of magnetic flux. Since these charged particles are the carriers for any current, it too can only flow along flux lines. Much lower down at 90-150 km from the surface the density of neutral particles is high enough that it causes a significant number of collisions. These collisions randomize the motion of the ions enough for conduction perpendicular to the magnetic field to be possible. Below 90km the density of charged particles decreases rapidly and, therefore, so does the conductivity. The layer of good conductivity in all directions located near 100km is important for understanding the auroral electrojet.

To a first order approximation the magnetic field of the Earth near the surface is that of a dipole. The magnetosphere is shaped both by this dipole magnetic field and by the solar wind (Cowley, 1995). The frozen-in magnetic field in the plasma of the solar wind compresses the Earth's magnetic field on the sun-ward side until the pressure from the solar wind is balanced by the magnetic pressure from the Earth's field, like the balance achieved when floating one magnet above another. This boundary is usually about 10 Earth radii from the centre of the Earth on the sun-ward side and is know as the magnetopause. Figure 2.4 shows the Earth's magnetic field. On the anti-sunward side the magnetotail is blown and extended out by the solar wind, and so extends tens of times as far as the magnetopause on the sunward side.

The solar wind produces a bow-shock when it collides with the Earth's magnetic field, much like a fast moving CME creates a shock wave when it encounters slower moving plasma (Suess, Tsurutani, 1998). The area between this bow-shock and the magnetopause is known as the magnetosheath and is populated with turbulent heated plasma.

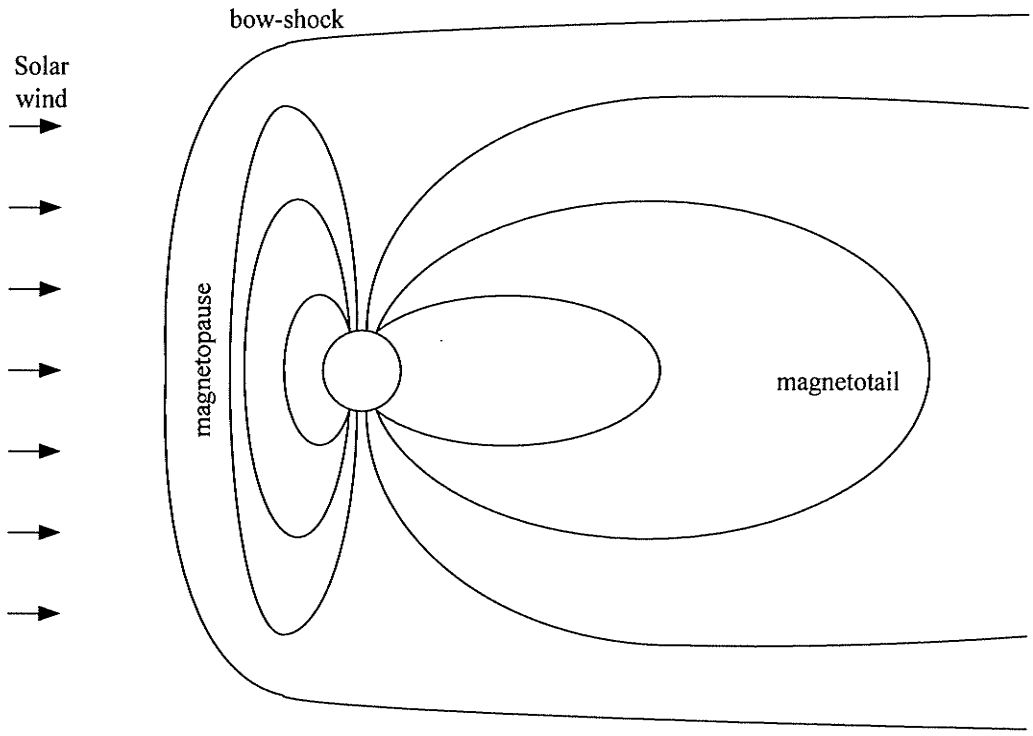

Figure 2.4 The Earth's Magnetosphere. Not to scale.

2.4 Interaction Mechanisms

The turbulent solar wind is constantly buffeting and deforming the magnetosphere. When studying geomagnetic effects the most important variable is the south-directed component of the solar wind's magnetic flux density ($-B_Z$).

There are several solar wind mechanisms described in section 2.2 that will allow the magnetic field of the plasma striking the magnetosphere to have a southern orientation, or negative value of B_Z, including magnetic clouds and Alfvén waves. If the orientation of the magnetic field of the solar wind is in the negative B_Z direction it is possible, but not inevitable, that a magnetic reconnection will occur (Tsurutani, Gonzalez, 1997).

A magnetic reconnection occurs when South-directed magnetic field lines from the sun connect to the North-directed field lines of the Earth through the magnetopause (Akasofu, 1992). This breaks apart the field lines around the Sun and Earth and "reconnects" them with each other. This allows the magnetopause to move toward the Earth and some of the solar wind to enter the magnetosphere. The open field lines are stripped from the day-side and blown around the poles of the Earth and join the long magnetotail on the night-side. The excess field lines in the magnetotail eventually pinch-off. The excess flux is blown into space and the Earth's field returns to a stable state (Cowley, 1995). Figure 2.5 shows a magnetic reconnection.

It is because of reconnections and the subsequent return to normal that the strongest geomagnetic perturbations occur (Campbell, 1997). As the magnetic lines of flux return to normal they move from their stretched position in the magnetotail back to their stable position on the sun-ward side of the Earth. This motion of magnetic flux has a dynamo effect which drives several current systems in the ionosphere, magnetosphere and the magnetotail. Of equal or even greater importance than the dynamo effect of the reconnection is the injection of plasma deep into the ionosphere that the reconnection allows (McPherron, 1997). Only the current systems which have the greatest effect on geomagnetically induced currents will be discussed here.

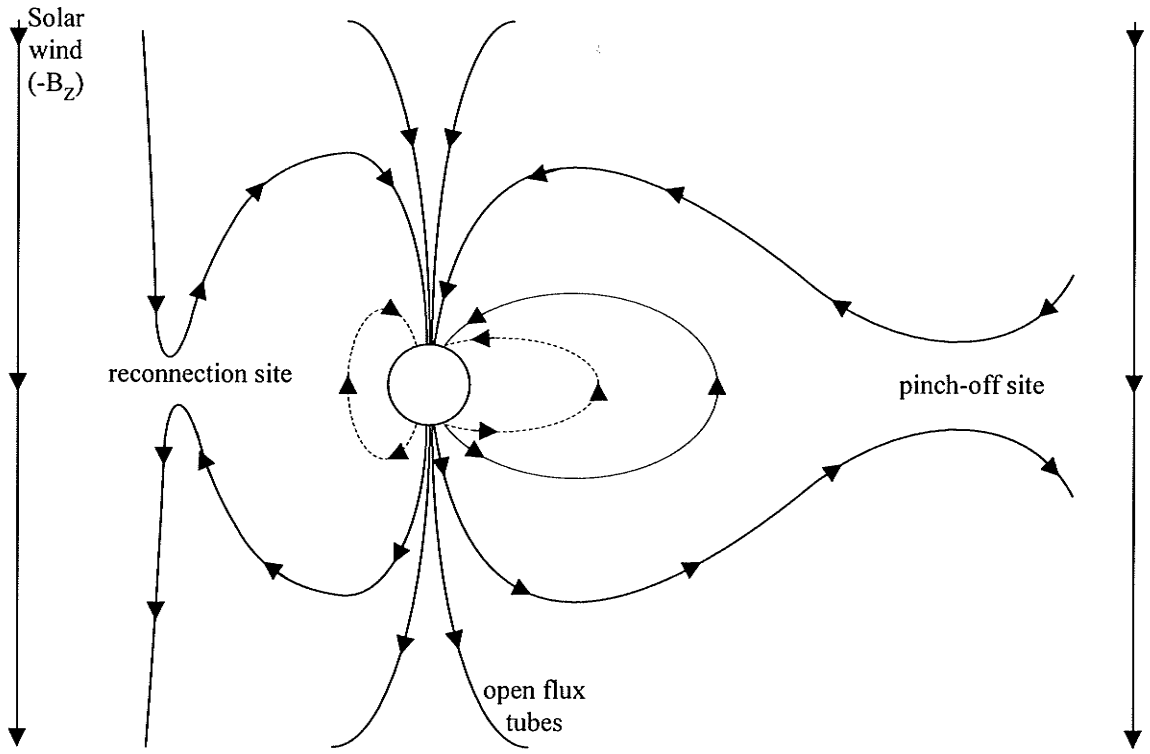

Figure 2.5 A South-directed magnetic field in the solar wind leads to reconnection and pinch-off.

When the Earth's pinched-off magnetic field returns, or snaps back, from its stretched position in the magnetotail it drags and heats plasma along with it (Tsurutani, Gonzalez, 1994). Some of this plasma follows magnetic lines of flux to the polar regions and is driven into the night time ionosphere and lower atmosphere where it excites the atoms of atmospheric gasses. These excited atoms emit light when they return to their stable energies. This light, which is seen as a glow in the night sky at high latitudes, is the aurora. Other plasma is forced deep into the night-time side magnetosphere. Here, various forces and effects (which are not well understood and will not be covered here) cause it to flow roughly around the equator as a number of different currents which are mostly directed to the West. The magnetic fields of the majority westward currents,

together known as the ring current, tend to oppose the main field of the Earth and it is this field change that defines a magnetic storm (Campbell, 1997).

Some of the Westward-directed ring current travels down magnetic lines of flux to the auroral-oval regions of the Earth, this is shown in figure 2.6. The auroral-oval is a variable band around each magnetic pole where the aurora are most often observed. The auroral-oval changes shape with changes in the solar wind and expands moving southward during magnetic storms (Daglis, 1997). The sheets of current driven down into the ionosphere and upper atmosphere create the characteristic curtain shape of the aurora. Once this current reaches the longitudinally conductive layer of the ionosphere it forms a large West-directed current know as the auroral electrojet. This current can be greater that 1 million Amperes and is the cause of geomagnetically induced currents at high latitudes. The current leaves the ionosphere along magnetic field lines and rejoins the westward currents in the magnetosphere. The reason for this detour is not clear, but is probably related to the reconnection process in the magnetotail (Suess, Tsurutani, 1998;Campbell, 1997).

The protective magnetosphere is not completely overwhelmed if the solar wind field is directed southward (-Bz). At most, the reconnection process only transfers 20% of the interplanetary flux directed at the Earth (Cowley, 1995). The rest is deflected around the magnetosphere. So, although important to the dynamics of the magnetosphere and ionosphere magnetic reconnections are not catastrophic for the Earth's shield against the solar wind.

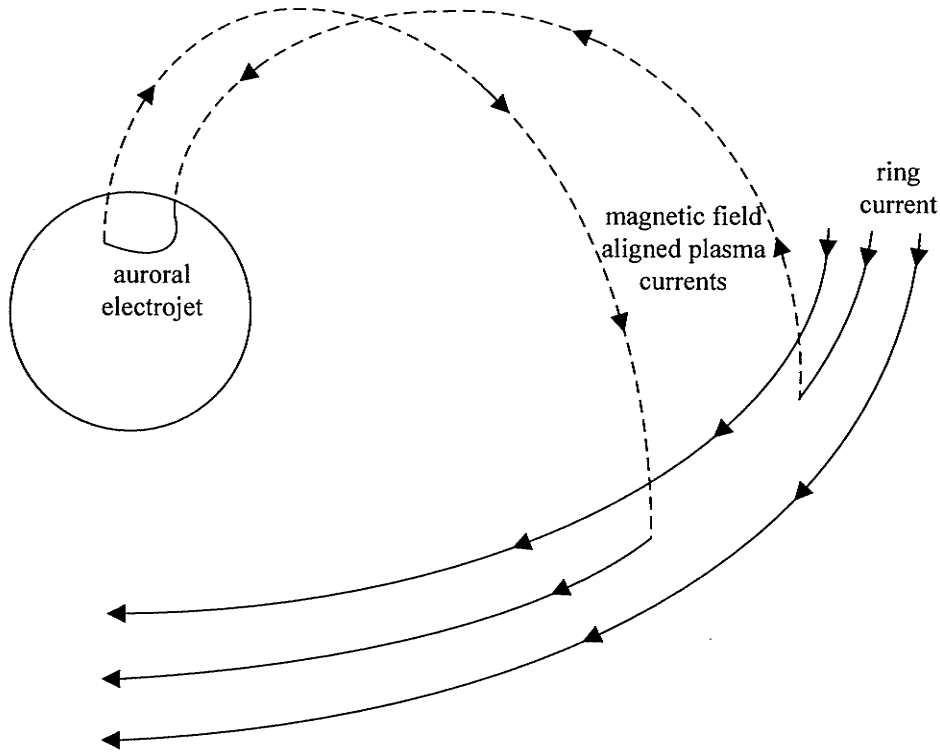

Figure 2.6 Current travels from the magnetotail along magnetic lines of flux to create the auroral electrojet.

The auroral electrojet is being caused by a complex and violent chain of events, and so it is highly variable in magnitude and position. This variability makes accurately modelling it and its effects on terrestrial systems extremely challenging.

2.5 Conclusion

The mechanisms of magnetic storms and substorms are varied, complicated and not well understood. This chapter has attempted to explain some of the better understood and most important mechanisms, based on the influence they have on terrestrial technological systems. The sun does not rotate as a rigid body. It moves faster near its equator than at its poles, and this differential motion complicates the magnetic field. The complicated and turbulent nature of the Sun's magnetic field is frozen-in to the interplanetary plasma that the Sun ejects. This plasma forms the solar wind which, in turn, has its own dynamic and complicated interactions. This magnetized solar wind blows against the Earth's magnetic field and deforms it from its dipole-like nature, forming the magnetosphere. The magnetosphere is a complex system of magnetic field lines, plasmas and currents that surround the Earth. The gusts and twisting of the solar wind and its magnetic field can weaken and disrupt parts of this system. These disruptions to the magnetosphere and their influence over the ionosphere, a layer of ionized gas in the upper atmosphere, are what cause the auroral electrojet which, in turn, induces currents on systems near the surface of the Earth.

Chapter 3

Electric and Magnetic Fields at the Surface of the Earth

3.1 Introduction

The first step in modeling the levels of GIC in a conductor or network is estimating the electric field at ground level. The fields of interest in this thesis are caused by current systems in the ionosphere, specifically the auroral electrojet. The electric and magnetic fields produced at the surface of the Earth by ionospheric current systems are very complicated and difficult to model. The fields are influenced by the shape, magnitude and motion of the ionosphereic currents above and by the structure of the Earth below the surface. Many simplifying assumptions must be made to create a practical model. This chapter describes the differences between uniform and non-uniform field models and compares the theory behind different solution methods.

3.2 Uniform Fields

Early calculations of the magnitude of current induced on transmission lines used uniform fields. These fields had been calculated as the upper limit of what the electric field could reach (Albertson, Van Baelen, 1970). To find the least favorable conditions at the surface of the Earth, the authors assumed a sheet current over the area of interest and calculated the fields by assuming a vertical plane wave.

This assumption resulted in strong and uniform fields. At the time, Albertson and Van Baelen recognized that this pessimistic uniform field method should only be used on isolated sections of transmission line and not entire networks.

3.3 Non-Uniform Fields

The uniform field model is not appropriate for studies of areas in the auroral region (Pirjola, Viljanen, 1989) where proximity to the electrojet would produce a very non-uniform field as shown in Figure 3.1. The auroral ovals move toward the equator, and more heavily populated areas, during strong geomagnetic storms when the effects are the most severe (Daglis, 1997). Because of this and the far reaching and non-uniform effects on surface electric field shown in Figure 3.1, the auroral electrojet should be modelled in as much detail as possible. This requires modelling the effects of non-uniform fields on networks.

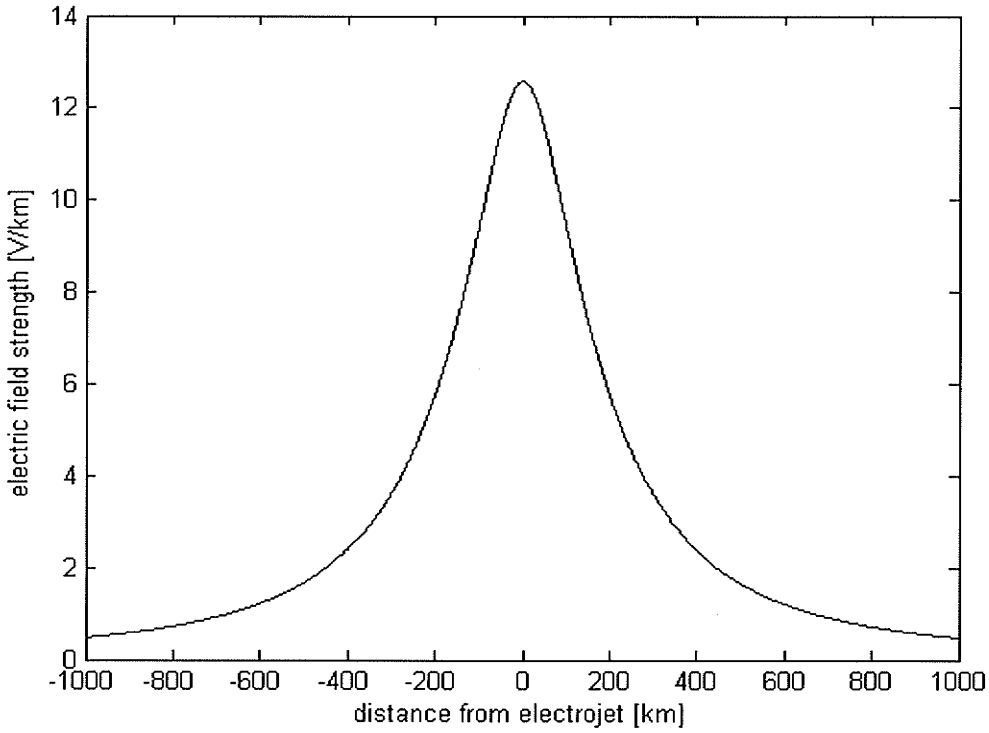

Figure 3.1 The Magnitude of the electric field strength as a function of the distance to the centre of an infinite current filament as calculated using the complex image method. A 1 MA electrojet with a 2 minute period was modeled 100 km above southern Manitoba.

In this thesis the auroral electrojet is modeled as an unmoving current filament with infinite length varying sinusoidaly at a single frequency. It is modeled over an infinite, multi-layer, flat earth. This model, shown in Figure 3.2, will produce more accurate results than the uniform electric fields traditionally assumed in North American studies of GICs on power systems (Boteler,Bui-Van,Lemay,1994. Boteler, Watanabe, Shier, Horita, 1982). Although not as realistic as more complex finite length or "U" shaped electrojet models (Pirjola, 1998), in this thesis the infinite current filament model is used as a compromise.

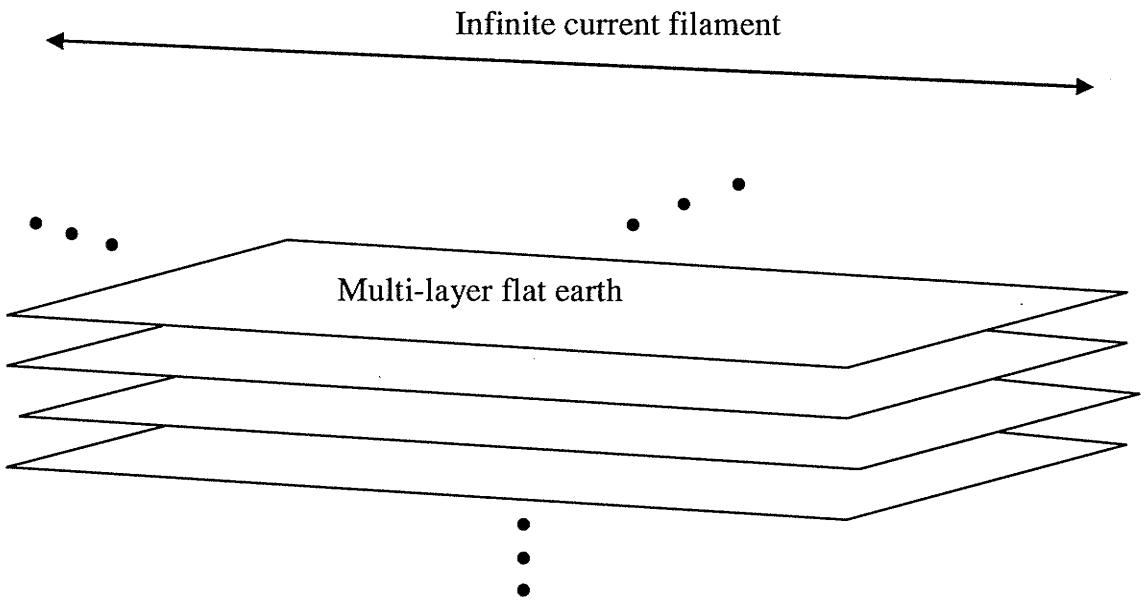

Figure 3.2 The Auroroal Electrojet is modeled as a current filament with zero width and infinite length over an infinite, flat, multi-layer earth.

The ground is modeled with a horizontally layered earth model described in Appendix A. Eight layers are modeled, each with a different depth and resistivity. The layered earth model is a reasonable first approximation of the Earth's structure where the area of study is not near an ocean boundary and is an improvement over studies that assumed a homogenous earth (Pirjola, 2002).

3.4 Relative Results

Pirjola and Viljanen's study on the Finnish 400kV system (1989) compares the results from uniform and non-uniform electric field models on a network. Even though the magnitude of the electrojet was adjusted so that the average electric field over the area of the network was 1 V/km in both cases, the study shows that uniform and non-uniform electric field models produce drastically different results. As one would expect, the average magnitudes of earth currents are similar but the non-uniform fields produce a much wider range of currents. Table 4.1 shows the results of Pirjola and Viljanen's simulation.

	GIC earthing current magnitude (A)	
Station Number	Uniform Field	Non-uniform Field
1	9.2	3.0
2	23.9	7.2
3	1.3	0.5
4	18.5	5.4
5	9.1	3.3
6	8.8	3.5
7	89.6	29.2
8	39.5	14.4
9	1.2	0.5
10	23.8	12.4
11	23.1	6.9
12	42.3	37.0
13	51.0	92.0
14	15.3	44.1
15	93.4	238.4
16	96.9	270.3
17	59.9	166.3
18	24.3	8.7
19	40.0	12.9
20	4.9	35.8

Table 4.1 GIC earthing current magnitudes in Finnish 400kV network under uniform and non-uniform fields with average electric field of 1 V/km. From (Pirjola, Viljanen 1989).

As most of Manitoba is in a typical auroral zone location (Campbell, 1997), modeling the auroral electrojet as a current sheet producing a uniform field would not be appropriate. The peak ground currents that are induced directly under or near the electrojet would be severely underestimated.

3.5 Calculation of the Electric Field Under a Current Filament

In order to calculate the voltage induced on transmission lines near the surface of the Earth it is first necessary to calculate the electric field produced by the electrojet. This thesis considers two options for this: the exact solution and the complex-image method.

3.5.1 Exact solution

In this context the exact solution refers to an exact solution of Maxwell's equations given a current filament of infinite length, varying sinusoidaly over a multi-layered earth. The solution involves solving Maxell's equations in the air and in every layer of the earth model with boundary conditions (Pirjola 2002). The formulas for the electric and magnetic fields at the surface of a two layer earth are given in Hermance & Peltier (1970). There the integral for the electric field is given as:

$$E_y = -i\omega\mu \frac{I}{2\pi} \int_0^\infty (1 - R) \frac{e^{-h\lambda}}{\lambda} \cos(\lambda x) d\lambda \qquad (3\text{-}1)$$

where R is the reflection coefficient given in Appendix A and λ is a constant of integration.

Even using judiciously chosen approximations, computers and advanced integration methods, the calculation of this integral is difficult and time consuming (Boteler & Pirjola 1998a).

3.5.2 The complex-image method

Introduced by Wait and Spies (1969), the complex image method is more sophisticated but similar in concept to the method of images used to calculate electric fields in power systems. The layered earth model is replaced by a perfect conductor at a complex depth below the surface. In their paper Wait and Spies begin with an exact equation for the electric field like equation 3-1 above, and using carefully chosen analytic techniques and simplifications develop a closed-form non integral equation for the electric field similar to equation 3-2 below.

Boteler and Pirjola (1998a) derived the equations for the electric and magnetic fields at the surface of the earth from an infinite current filament using the complex image method. Results from their formulation were then compared to results obtained using the exact solution and found to be in excellent agreement over two different layered earth models for line current parameters that are typical of auroral electrojet behaviour. The small differences in the results produced by the two methods are easily acceptable when one considers the uncertainty in the magnitude and location of the electrojet and the

approximations in the layered earth model. In reality, the use of the much simpler complex image method will have no influence on the accuracy of the model.

Because of its simplicity and accuracy, the complex image method of Boteler and Pirjola (1998a) is used in this thesis. Wait and Spies showed that the complex image method was analytically sound and Boteler and Pirjola showed its accuracy for electrojet studies. The only one of Boteler and Pirjola's calculated fields needed to calculate the induced voltage along a transmission line, the electric field parallel to the electrojet, is simplified to:

$$E_y = -\frac{j\varpi\mu_0 I}{2\pi} \ln\left[\frac{\sqrt{(h+2p)^2 + x^2}}{\sqrt{h^2 + x^2}}\right] \qquad (3\text{-}2)$$

where "h" is the height of the electrojet, "x" is the lateral distance and "p" is the complex depth. Figure 3.3 shows a physical representation of some parameters from 3-2.

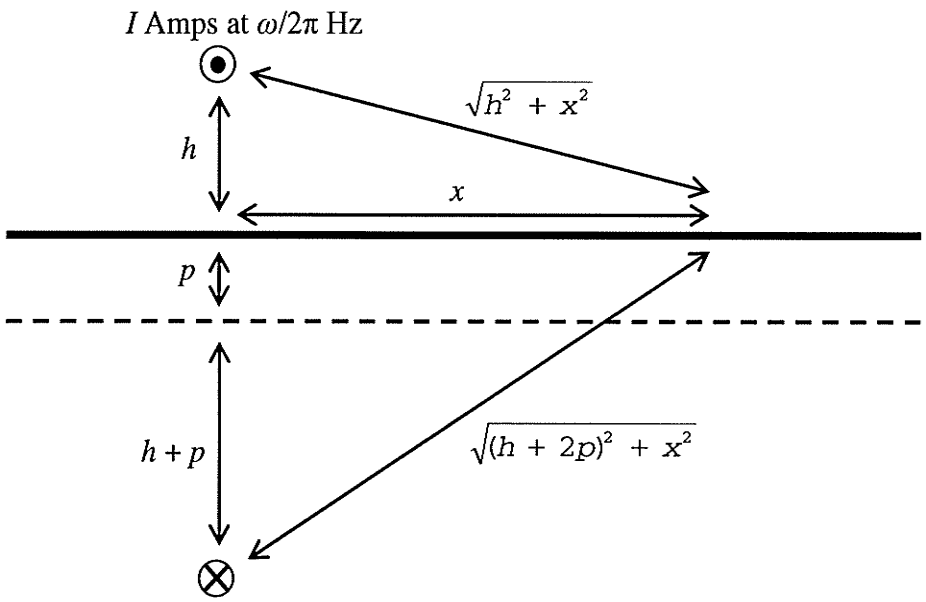

Figure 3.3 Representation of terms from complex image calculation of electric field parallel to an infinite line current

The complex depth p is found using the following:

$$p = \frac{Z}{j\varpi\mu_0} \tag{3-3}$$

where the calculation of the surface impedance (Z) of the layered earth model is given in Appendix A.

3.6 Conclusion

It is suggested that for studies of networks at auroral latitudes treating the electrojet as a current sheet, leading to a uniform electric field, is not ideal. In this thesis the electrojet is therefore assumed to be an infinite, unmoving current filament varying at a single frequency.

Exact and complex image methods of calculating electric fields were discussed. The complex image method provides a simple equation for the calculation of the fields caused by the electrojet at the surface of the Earth. The results obtained from these methods are almost indistinguishable from the exact solution, and are therefore very easily within the error and uncertainty in many of the other assumptions made in modeling the electrojet (Boteler, Pirjola, 1998a).

Chapter 4

Modeling GIC in a Network

4.1 Introduction

The geomagnetically induced currents in the transmission lines are not of concern to power utilities. It is when these currents flow through the ground connections of power transformers that problems are caused. These transformers are located at stations where several transmission lines can be connected. Because the GIC in transformers can be caused by several lines and is dependant on system configuration (Boteler, 1994) the network beyond the station being studied should be modeled.

People in the power systems field have long used Earth-Surface Potentials (ESPs) to explain and model GICs (Albertson, Thorson, Miske, 1974, EPRI, 2002). Geomagnetically Induced Currents flowing in transformer neutrals are said to be caused by potential differences along the surface of the Earth between the grounding points. The currents are modeled by inserting voltage or current sources at the ground connections of transformers. When modeling a conductor, or network of conductors, in a uniform field this method can produce consistent results. However, the more realistic non-uniform non-conservative fields produced by the electrojet model used in this thesis require the use of in-line voltage sources to model induction onto transmission lines. Boteler and Prijola (1998b) compared the modeling of GIC produced by uniform and non-uniform

electric fields. Sections 4.2 and 4.3 of this thesis are based on their examples and analysis. This chapter shows the necessity of using in-line voltage source modeling when representing non-uniform electric fields.

4.2 Modeling GICs in Uniform Electric Fields

Uniform fields are conservative and the influence of these fields on a discreetly grounded transmission system can be represented by introducing voltages in the grounding points or by using in-line voltage sources. This is best demonstrated by example.

The simple transmission system shown in Fig. 4.1 consists of 4 transmission lines, each 100 km long, and 4 transmission stations. The transmission lines form a perfect square and are aligned either North-South or East-West. The stations are at each corner.

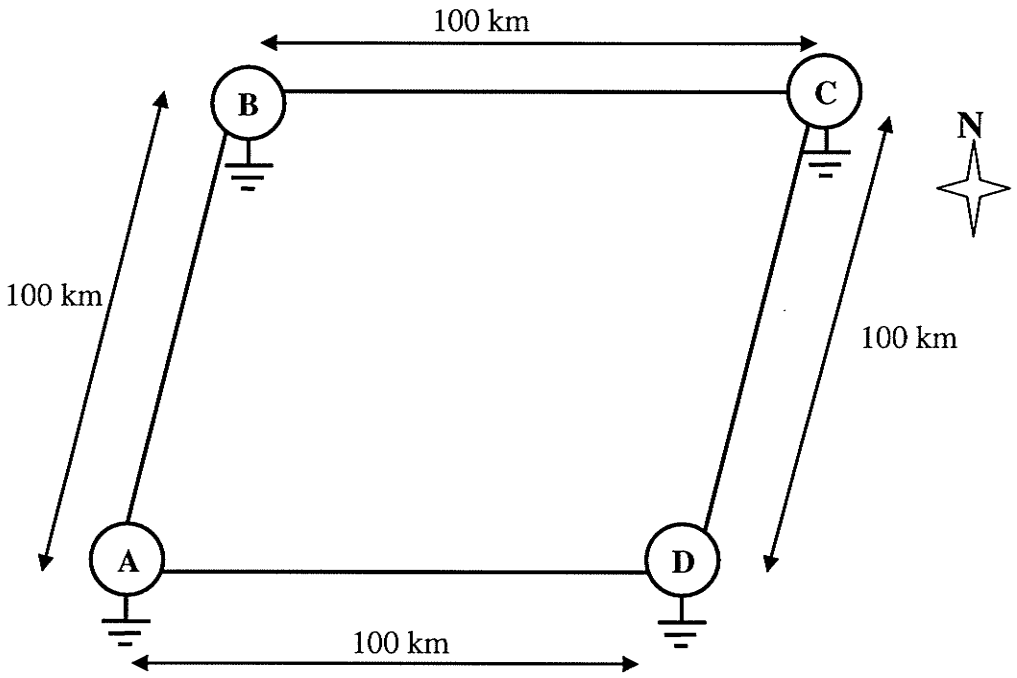

Figure 4.1 Simple transmission network 4.2.2 in-line voltage source

4.2.1 Earth surface potential

If we assume a uniform electric field of 1 V/km along the East-West axis the difference in potential between points A-D and B-C will be 100 V. There is no potential difference between A-B and C-D.

As shown in Fig. 4.2, this can be represented with a single 100 V source in the ground connection of two stations, with the other stations simply grounded.

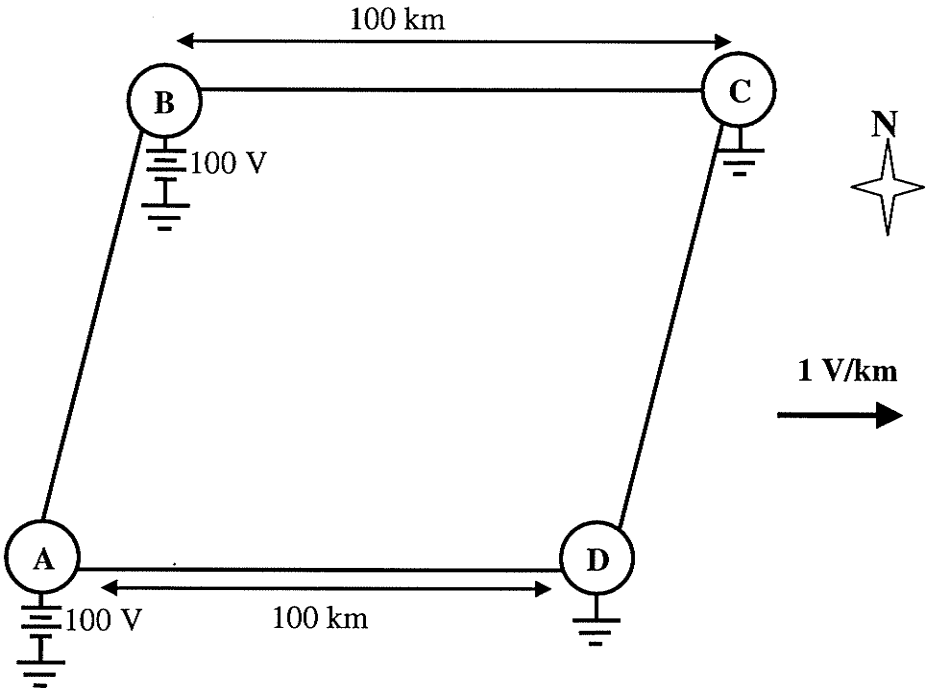

Figure 4.2 Representation of uniform field with Earth surface potentials.

4.2.2 In-line voltage source

If we assume a uniform electric field of 1 V/km along the East-West axis the line sections A-D and B-C each develop 100 V while the other line sections follow equipotential lines and develop no voltage.

The voltage along the East-West lines can be modeled by inserting 100 V sources in series with them, as show in fig. 4.3. The resulting voltages and currents will be identical to what was produced using sources in the ground connections.

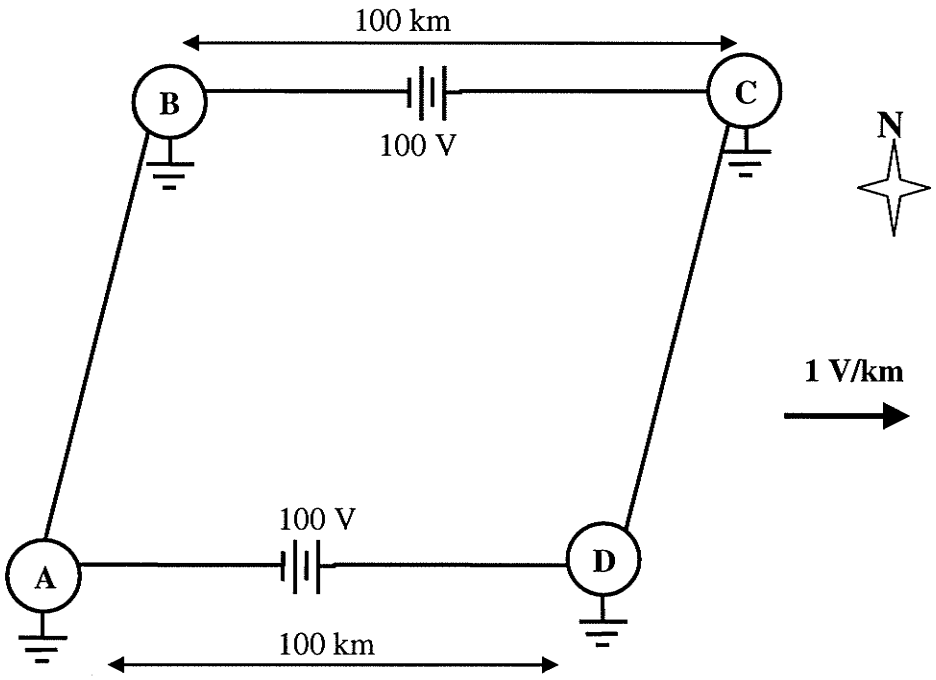

Figure 4.3 Representation of uniform field with in-line voltage sources.

4.3 Modeling GICs in Non-Uniform Fields

More realistic models of the main driver of GICs, the auroral electrojet, create non-uniform non-conservative fields. In the case of the infinite line current model used in this thesis, the electric field is directed parallel to the electrojet current, strongest directly under the electrojet, and decreases in strength with perpendicular distance.

Considering the system of fig. 4.1, an East-West oriented electrojet will most likely be closer to one of the East-West transmission lines, say B-C, than the other. This will cause a higher electric field between B and C than appears between A and D. The 100 V first-order approximation is retained but a variable x is used to represent the electric field non-uniformity.

4.3.1 Earth surface potential

In this case, following the procedure of adding voltage sources in the grounds of stations that worked for the uniform field does not represent the system. It models an induced potential difference where there should be none. The erroneous potential appears across A-B and is equal to 200x. The situation is shown in fig. 4.4. It is important to note that in systems with finite ground resistances there may be a potential difference between points A and B, but this difference is caused by different magnitudes of current being driven into the ground resistance and not by induction. That potential difference must therefore be handled as part of the circuit simulation and not as part of the induction modeling.

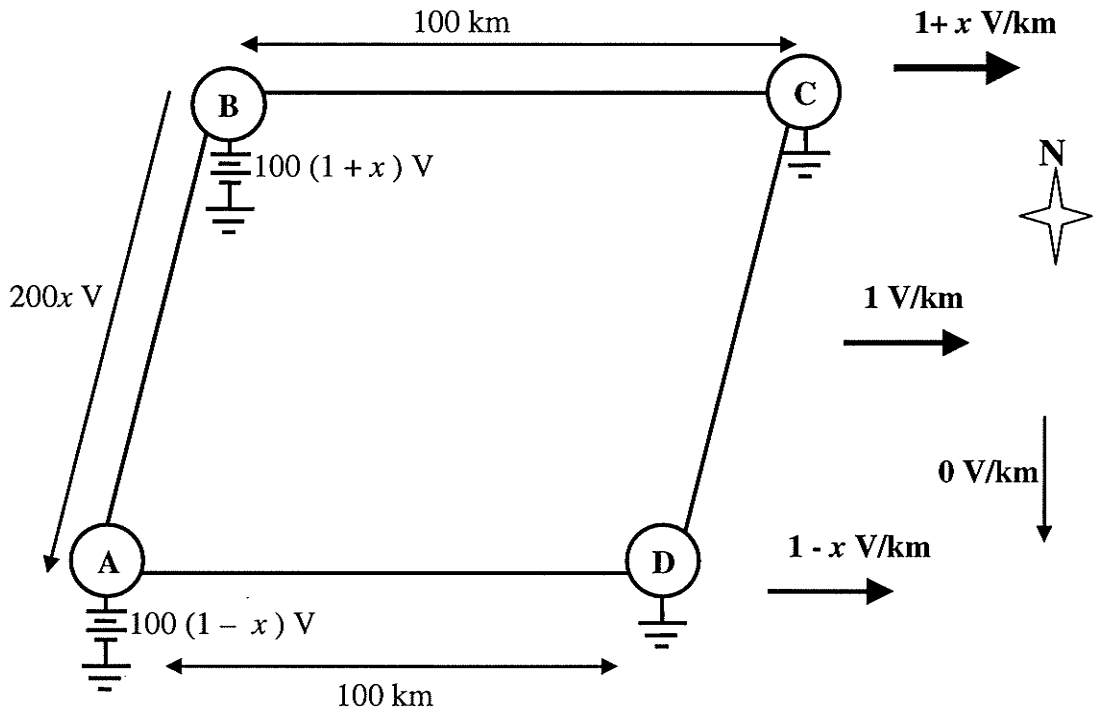

Figure 4.4 **Representation of non-uniform field with Earth surface potentials. Note that a North-South voltage appears in the grid although there is no North-South electric field.**

An example of incorrectly using ground sources is described in Albertson, et al. (1981). In this paper they attempted to use ground sources to model GICs within a load flow program. The overall electric field was not uniform and was modeled as several zones, with a uniform field within each zone. Similarly, Prabhakara et al. (1992) use Earth surface potentials in a load flow program that had been calculated from a non-uniform field model (Towle et al., 1992). The idea that GICs are caused by Earth surface potential differences, and therefore that this is an appropriate way to model them, is deeply ingrained in the power system community.

No combination of reference points and grounded voltage sources is able to correctly represent a network in a non-uniform field (Boteler, Prijola,1998b). It is also important to note that the results from a grounded source model are not unique. If node A had been chosen as the reference node, the spurious North-South current would have been between nodes C and D instead of A and B. Since the choice of reference node is theoretically arbitrary, the fact that its choice changes the currents at the nodes clearly shows a serious problem with using grounded sources to model non-uniform fields.

Physically, the currents that flow in transmission lines are not caused by Earth surface potentials, rather they are both caused by induction from the same phenomenon. The electrical characteristics of the earth underneath the transmission line do influence the magnitude of induced GIC, but in the same way a resistor in parallel with a wire influences how much current flows in each: it offers an alternate path.

4.3.2 In-line voltage source

Shown in fig. 4.5, in-line voltage sources can represent the non-uniform field accurately. The in-line sources make it possible to represent path dependence, which is essential in modeling non-conservative fields. Using Earth surface potentials it is impossible to create even a relatively simple network, like those shown, that can accurately represent the induction caused by a non-uniform field. Since the infinite current filament that is being used to model the auroral electrojet produces a non-conservative field, a model

using in-line sources is required. There is no arbitrary choice of reference node when using in-line voltage sources and the solution is unique.

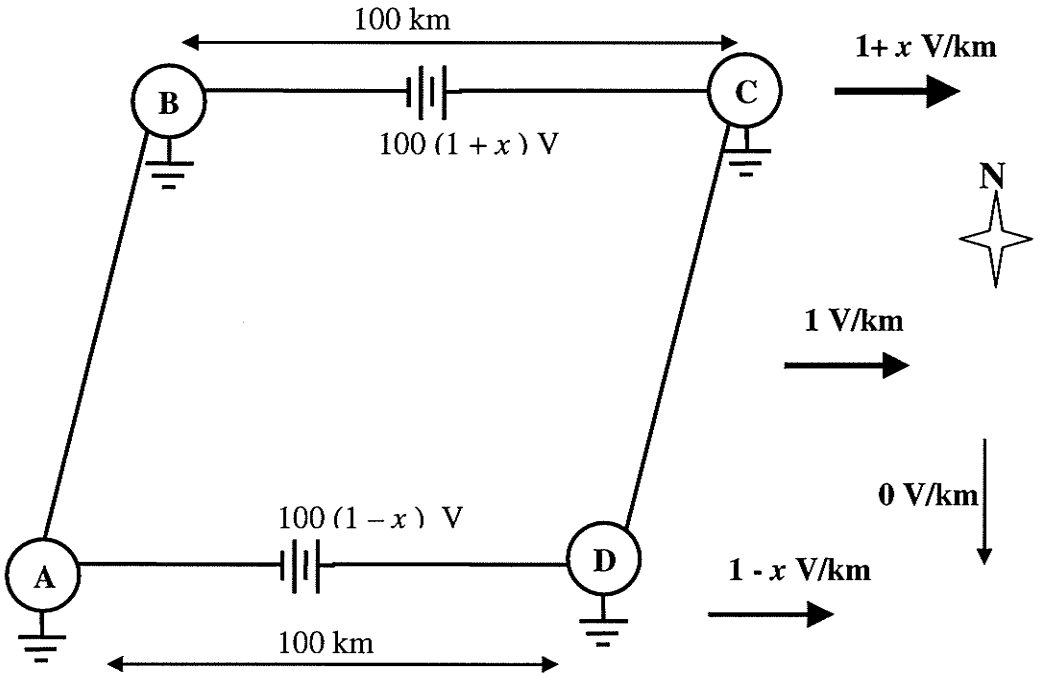

Figure 4.5 Representation of non-uniform field with in-line voltage sources.

4.4 Conclusion

The flawed Earth surface potential concept has been used for a long time in the power system field and remains a common explanation for the GIC phenomenon (Price, 2002). Modeling GICs using this concept is not compatible with the non-uniform fields predicted by the more accurate electrojet models required when studying GIC effects at high latitudes. In order to correctly model the behaviour of a network under the influence of an infinite line current, in-line voltage sources must be used.

Chapter 5

Calculation of Induced Voltage

5.1 Introduction

The voltage induced on a transmission line must be calculated before it can be used in a network model. A more accurate method for calculating the induced voltage is one of the main features of this thesis. The more accurate values for the induced voltage are possible because the electrojet is modeled as an infinite line current instead of a sheet current. This increased accuracy comes at the cost of additional complexity as the electric field at the surface of the earth caused by the line current is non-uniform and forms a non-conservative vector field. The locations of the transmission line end-points are therefore not sufficient to calculate induced voltage, and the paths of the transmission lines under the electrojet must be considered. This requires coordinated geographic information about the locations and paths of transmission lines in the network. The relationship between the transmission lines and the electric field under the electrojet is determined by using AutoCAD .DXF files containing coordinated mapping data of the transmission lines, and fixing the location and orientation of the electrojet. The complex image method is then used to calculate the electric field at any point desired. A line integral of the electric field along the path of each transmission line must be performed to find the total induced voltage on that line. This must then be repeated for each line in the modeled network. These calculated voltages can then be used in a realistic model of the network.

5.2 Geographic Data

This thesis uses AutoCAD maps of the transmission line routes. These maps must use the UTM (universal transverse Mercator) system. This system approximates the Earth's surface as a grid of thin slices. Each slice, called a zone, is assigned a unique number and Cartesian coordinates are used within the zone. The zone number and the coordinates within the zone allow a unique identification of each point on the surface of the Earth. (Dana, 1999) Most of Manitoba falls into a single zone, 14N.

AutoCAD drawing flies (.DWG files) can be converted into Autodesk's drawing exchange format (these files have .DXF extensions) (Autodesk, 1997). The drawing exchange format allows any program capable of reading text to extract geographic information from the files. The DXF files are separated into sections and use numerical codes, called group codes, to organize the information required to reproduce a drawing. The section in the file and the group code that precede a value dictate exactly what that value represents. For the purposes of this thesis the only section of interest is the "ENTITIES" section of the file which contains information about the actual objects that appear in the drawing. This section contains the Cartesian coordinates of whatever the file is illustrating. In the case of transmission line maps the transmission lines are represented by many line segments. The "ENTITIES" section contains the UTM coordinates of the beginning and end points, or definition points, of each line segment. The x coordinate of a definition point follows the group code "10" and the y coordinate follows a "20". The DWG file is searched for the "ENTITIES" section and then the section is searched for "10"s and "20"s with the values after these group codes recorded

as transmission line coordinates. By reading the locations of each definition point the ends of the line segment are known and the path of each transmission line can be determined.

5.3 Electric Field Data

In addition to the locations and paths of the transmission lines, the location and orientation of the electrojet is also required to calculate the induced voltage. In this thesis the location and orientation of the electrojet is defined mathematically by a single UTM coordinate pair (x,y) and a heading in degrees east of true north. With this information the perpendicular distance from the electrojet to any point in the zone can be calculated with following formula:

$$d = \left|\cos(\gamma)\{[cy + \tan(\gamma)\,(x - cx)] - y\}\right| \qquad (5\text{-}1)$$

Where γ is the angle of the electrojet from the x, or East-West axis, cx and cy define any point directly under the electrojet and x and y are the coordinates of the point of interest. The result, d, is the perpendicular or lateral distance to the electrojet from the point of interest.

The derivation of this formula, a diagram depicting it and justification for using Cartesian mathematics on the surface of a curved sphere appear in Appendix B.

With the perpendicular distance to the electrojet, the electric filed strength can be calculated using the complex image method described in section 3.4. Alternatively, if a uniform field is desired for comparison, a fixed value for the electric field can be used instead of the complex image calculation. The orientation of the field is still defined by the angle of the electrojet that is input into the subroutine but the distance between the transmission line segment and the centre of the electrojet will have no effect on the electric field strength.

5.4 Line Integral

The magnitude of the induced voltage in an arbitrary electric field can be found by integrating the dot product of the transmission line vector and the electric field vector at the ground along the path of the transmission line.

$$V_{AB} = \int_{A}^{B} \vec{E} \bullet d\vec{l} \qquad (5\text{-}2)$$

Where V_{AB} is the voltage driving current from point A to point B, E is the electric field on the ground and dl is the differential element of the transmission line between A and B.

This integral is the fundamental definition of the potential difference between two points as work per unit charge (Cheng, 1989) and in this application it neatly takes the length and orientation of the line with respect to the electrojet into consideration and accurately calculates the induced voltage.

5.5 Numerical Integration

Integration along the line is accomplished by splitting each of the transmission line segments (read from the .DXF file) into n subsections. The electric field in the subsection is calculated as the average of the electric fields at the endpoints of the subsection and is assumed to be uniform over its length. The dot-product calculations are then performed on each of these subsections and then summed over the whole segment. For each sub-section the following formula is used to calculate the dot product portion of the line integral (Sadiku, 1994):

$$V_{ss} = \Delta x E \cos(\gamma) + \Delta y E \sin(\lambda) \qquad (5\text{-}3)$$

Where γ is the angle of the electric field measured clockwise from East, E is the magnitude of the electric field in the subsection, Δx and Δy are the x and y components of the subsection and V_{ss} is the approximate voltage induced on the subsection. The segment voltage is found using:

$$V_{seg} = \sum_{i=1}^{n} V_{ss\,i} \qquad (5\text{-}4)$$

This procedure is repeated for each segment to find the total induction on the transmission line and the total line voltage is:

$$V_l = \sum_{i=1}^{n} V_{seg_i} \qquad (5\text{-}5)$$

This value is then passed into the electrical model of the network in PSCAD.

5.6 Incorporation into PSCAD

PSCAD is a time-domain power system simulation software package from the Manitoba HVdc research centre. With this software it is possible to create user-defined page components and incorporate them into the simulation. For this thesis such a component was created. A FORTRAN subroutine called Vin.f, included in APPENDIX C, was written which would calculate the surface impedance of the earth under a transmission line, calculate the complex depth, open and read a specified .DXF file, extract geographic information about the location and path of the transmission line, calculate the electric field along the transmission line resulting from a specified infinite line current and integrate the resultant electric field along the path of the transmission line. This induced voltage is returned via the user-defined component to the PSCAD environment where it can be used as an input to in-line voltage sources in network models.

Since the voltage sources in PSCAD require that the input voltage be given in RMS the result from the calculations in Vin.f are divided by $\sqrt{2}$ to compensate. Unfortunately the sign of the voltage depends on the direction of integration along the path, and so depends

on the direction in which the line segments appear in the .DXF map file. Since this order is arbitrary as far as AutoCAD is concerned it is possible for conflicts to occur. On reasonable sized systems the incorrect sign on the voltage would not be difficult to find and correct. The sign can be easily changed within the PSCAD environment in a number of ways, including multiplying the signal by -1, changing the phase by 180 degrees or, preferably, by changing the orientation of the voltage source component. Rotating the voltage source component is the most illustrative way in the graphical user environment to show that the induction on that transmission line has been calculated in the opposite direction. In this thesis the paths of the transmission lines were manually checked and the voltage sources in the graphical environment were oriented to match, which ensured the correct voltage would be introduced into the network. It is possible to eliminate the requirement to manually check the paths of the transmission line by performing a check within the voltage calculation subroutine. This is suggested as a possible future development.

5.7 Conclusion

The electric fields at the surface of the Earth are modeled as non-uniform in this thesis. Because of this the paths of the transmission lines need to be modeled in detail. This has not been the case with other, more simple, GIC studies. A program was created to combine geographic assumptions about the auroral electrojet and detailed maps of transmission lines to calculate the total voltage induced in the transmission line. These induced voltages can then be passed into a PSCAD simulation for incorporation into a network model.

Chapter 6

PSCAD Network Models

6.1 Introduction

PSCAD is a popular commercial software package for time-domain power system simulation. PSCAD was used to create a custom graphic that could be used in the Graphical User Interface (GUI) to execute custom FORTRAN code. A simple resistive network was chosen to study the induction of GICs onto a network. Because the typical frequencies of GICs are much lower than the 60 Hz that power systems are designed for, they would tend to behave as though a power system network were purely resistive. A simple network would remain easy to understand but would still show the difference between the in-line source and the ground source models. Figure 6.1 shows a representation of the basic network. To model GIC on this network two cases were created: one with in-line sources and one with ground sources. Multiple simulations were then carried out on each network with the angle of the electrojet changing in each simulation. PSCAD is not required to model such simple networks, but incorporating the voltage calculation component into a power system simulator is intended to make future developments possible. This chapter describes the integration of an induced voltage component and modeling of a simple network in PSCAD.

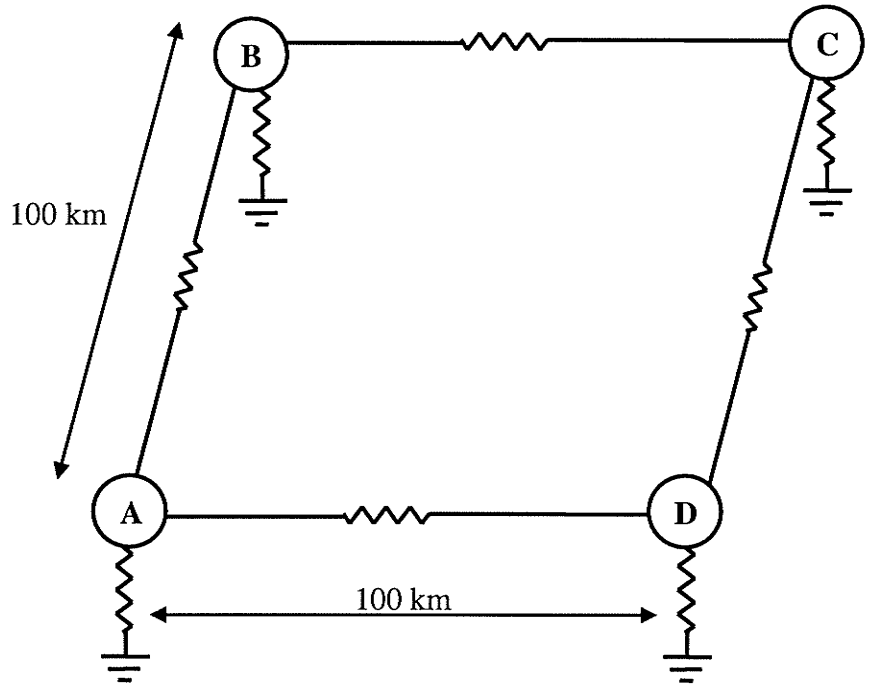

Figure 6.1 A representation of the basic network being studied.

6.2 Page Component

Inside PSCAD it is possible to create custom page components that allow users' custom FORTRAN code to be executed and interact with other power system components in the PSCAD GUI (Manitoba HVDC Research Centre Inc., 2004). A page component that calls the voltage calculation subroutine Vin.f, described in chapter 5 was created.

6.2.1 Script

The script that calls the voltage calculation subroutine was written so that the voltage calculations are only performed at the beginning of each PSCAD simulation run. This FORTRAN script, which is also included in Appendix C, makes the simulations much faster by preventing the induced voltages from being recalculated at each time-step. This feature makes it impossible for the output of the page component to change once the simulation is running; it remains constant even if the electrojet parameters are changed. At first this may seem inconvenient but it is necessary as well as useful for speeding the simulations. The calculation of the induced voltage is done in the frequency domain, and the frequency of the electrojet is one of the input parameters passed to the voltage calculation program. If the other parameters of the electrojet were changeable in the time-domain PSCAD simulation the frequency passed to the induction subroutine would need to change. This input parameter would have to be calculated from the rate of change of the other parameters in each time-step before it was passed to the subroutine. This could become extremely complicated. For example: If the electrojet was rotated about a fixed point (which involves changing only one input parameter, the heading) the current would posses a rate of change not only along its path but a separate rate of change perpendicular to, and varying along, its path. Calculation of the voltage induced on transmission lines under these conditions is beyond the scope of this thesis and is not required to study the electrojet configurations discussed in section 6.5.

6.2.2 Variables

The PSCAD page component for calculating the induced voltage along a transmission line is called Vin. The component has one binary and 6 real inputs whose values are passed to the voltage calculation subroutine Vin.f. One real output is produced and passed from Vin.f back to the GUI through the output node of the page component. The names of the variables in the page component, their types and their functions are listed in Table 6.1.

Name	Type	Definition
I	real input data	electrojet current [A]
f	real input data	electrojet frequency [Hz]
h	real input data	electrojet height [m]
cx	real input data	UTM x-coordinate directly under electrojet
cy	real input data	UTM y-coordinate directly under electrojet
ang	real input data	angle of electrojet from true North
north	logical input data	northern or southern ground model
V	real output data	induced voltage on transmission line

Table 6.1 Name, type and definition of variables in the Vin page component.

6.2.3 Parameters

Page components can also include adjustable parameters. These can not be passed directly from, or to, other components in the GUI, but can be accessed and changed by the user by double-clicking on the page component graphic. There are 2 parameters that can be adjusted in the Vin page component. These parameters are the number of sub-sections that each transmission line segment is split into for numerical integration and the

location and name of the .DXF file containing the transmission line map. Adjusting the number of sub-sections that each section is divided into will affect the speed and accuracy of the result. This parameter can be fine tuned depending on the length of the subsections in the .DXF file. Transmission lines with torturous routes tend to be split into smaller line sections and these shorter sections may require fewer subsections to achieve a desired level of accuracy. The results for most transmission lines are not particularly sensitive to this parameter and the default value of 1000 sub-sections provides acceptable accuracy and speed. A map of each transmission line is required to calculate the voltage induced on that particular transmission line under the non-uniform electric field. These values are passed by the page component script to Vin.f as an integer "n" and a string "filenm" and are needed to calculate the voltage induced on the line.

6.2.4 Graphic

Figure 6.2 shows the, admittedly utilitarian, PSCAD graphic that provides a platform for the variables to be input into the Vin.f code directly from the GUI and allows the calculated voltage to be sent directly to voltage source components in PSCAD. The output induced voltage, which has been converted to RMS by Vin.f, is output and can be connected to standard PSCAD voltage sources.

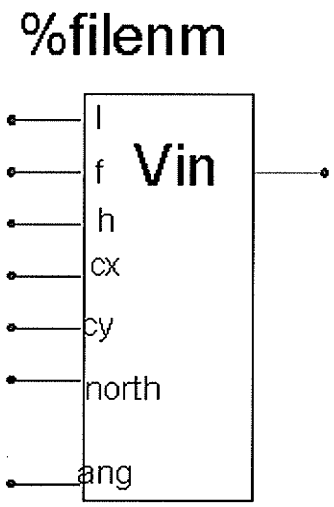

Figure 6.2 Graphic for custom PSCAD page component Vin. In the PSCAD environment the location of the transmission line map file appears where the figure shows "%filenm".

6.3 Simple Network for Ground Sources

Figure 6.3 shows the PSCAD representation of the network built to find results with grounded sources representing the induced voltages driving GICs. Station D is arbitrarily chosen as the reference ground. For uniform fields this choice makes no difference. Under realistic non-uniform fields different results are produced with the choice of any other stations as the reference ground, but there is nothing to favor one station over another. As described in section 4.3.1 in chapter 4, the solution under realistic fields is not unique. Station A has 2 voltage sources as a result of grounding station D. One voltage source represents the voltage from the North-South directed transmission line number 1 and the other represents the East-West directed transmission line number 2. The voltages applied by the sources are those calculated for each of the corresponding transmission lines.

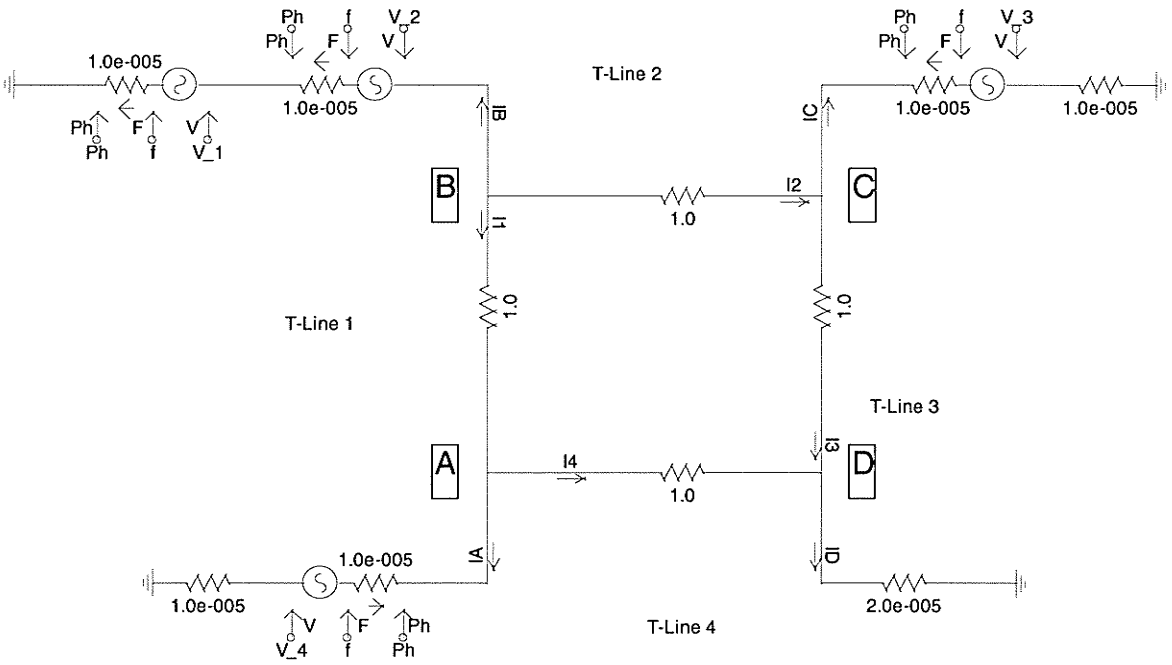

Figure 6.3 A network using grounded sources to drive simulated GICs. Station D is arbitrarily chosen as the reference ground.

The transmission lines are modeled as 1 Ω resistances and each source is in series with a 10 μΩ resistor. This requires an additional 10 μΩ resistor at stations with only one source and a 20 μΩ resistor at the ground reference station to maintain symmetry. Because of the long periods used for electrojet modeling the phase on the sources is adjusted so they begin the simulation at 90 degrees. This allows the maximum induced currents to be observed with short simulation runs. The voltage inputs to the sources are generated by 4 instances of the Vin page component which are shown in figure 6.4, each linked to a different transmission line map. The input variables are all common, with the exception of the ground model option, because each component is modeling the effect of the same electrojet on the different transmission lines.

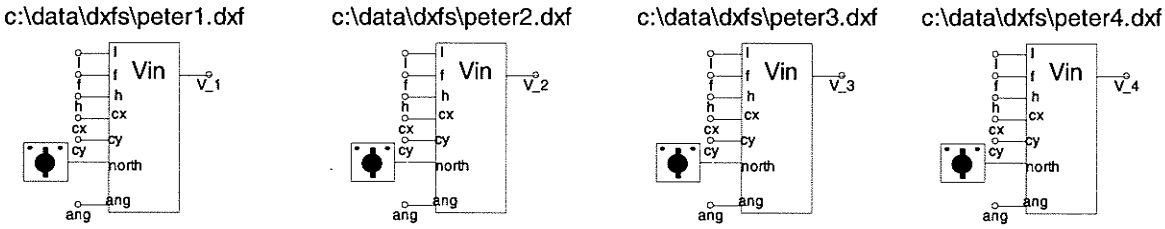

Figure 6.4 One Vin page component is required for each transmission line and provides an input voltage to one source. The common inputs describe a single electrojet.

6.4 Simple Network for In-line Sources

A very similar PSCAD model was created to represent the induced voltages as in-line voltage sources. The GUI representation is shown in Figure 6.5. The same resistances are used in each branch and the grounds as the ground source model so direct comparisons can be made. The orientation of the voltage sources is determined by the order in which the transmission line segments appear in the map file. Integration along a path in a vector field is not only path dependant but also direction dependant and the direction of the voltage sources was adjusted manually to account for that.

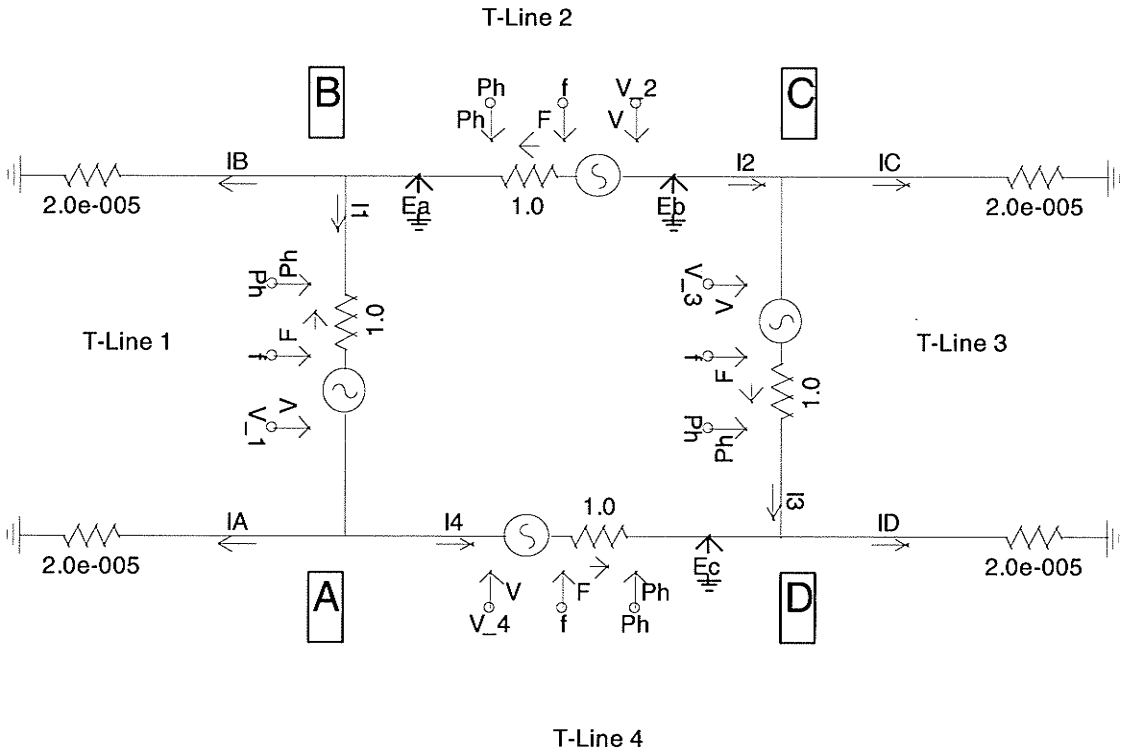

Figure 6.5 A network using in-line voltage sources to drive simulated GICs.

6.5 Multi-Run Simulations

A very powerful tool in the PSCAD program is the ability to automatically adjust parameters and perform multiple simulation runs automatically. The results from selected measurements can be automatically recorded in an output file for future reference.

In the simulations for this thesis the Multi-Run component was set to adjust the angle of the electrojet by 15 degrees between 0 and 180 degrees from true North. The readings of ammeters placed on each grounded leg of the network were recorded in an output file for further comparison. The results are given and discussed in Chapter 7.

6.6 Conclusion

With its ability to incorporate user FORTRAN code into a GUI, model in-line voltage sources in power system simulations and perform multi-run analyses, PSCAD is a convenient platform for modeling GIC induction. A page component for incorporating a subroutine for calculating voltage induced along a line from a given electrojet was built and two different simulations were created to compare results. The simulations each modeled a possible interpretation of the effects of induced voltage. One modeled ground potential rise on a simple network and the other modeled voltage induction along the transmission lines. Multi-run cases in PSCAD allow more detailed analysis (changing angle, location or any other parameter) than previous studies have attempted. The results and discussion of such analysis is given in Chapter 7.

Chapter 7

Results

7.1 Introduction

An experiment was performed to confirm the differences between in-line and grounded voltage source models. A subroutine to calculate and insert the voltages resulting from a uniform electric field was written. The routine described in chapter 5 was provided with realistic electrojet parameters to create a non-uniform and realistic electric filed. Two transmission networks were modeled with identical spatial characteristics, one using in-line voltage sources and the other using grounded sources. The ground currents of the each of the networks were calculated with each of the electric field models at a variety of orientations. The resultant ground currents show that grounded voltage sources are unable to represent the conditions under a non-uniform electric field.

7.2 Uniform Electric Field

A uniform electric field was modeled by using a modified version of the voltage calculation subroutine described in chapter 5. For simplicity, and because it has been used for other studies of directional sensitivity (Boteler, Bui-Van, Lemay, 1994), a value of 1 V/km was used for the uniform field. Because the purpose of the uniform field in this thesis is to show the grounded and in-line voltage sources producing the same results, the magnitude of the field and the resultant currents are not of significant interest.

7.3 Electrojet Model

Table 7.1 shows the parameters of the electrojet used to compare the effect of non-uniform, realistic electric fields on networks using in-line voltage sources with those using grounded voltage sources.

Parameter	Value used
Magnitude	1 000 000 Amperes
Frequency	0.0083333 Hertz
Height	100 km
Position	x: 556377 y: 5644491
Ground model	Southern
Orientation	0-180 degrees (in 15 degree steps)

Table 7.1 Electrojet parameters

7.3.1 Magnitude

The magnitudes of the induced network currents are directly proportional to the magnitude of the electrojet. Although the absolute magnitudes of these currents are not important for showing the importance of using in-line voltage sources, a realistic value for the electrojet was used. For the following experiments a peak electrojet current of 1 million Amps was used. This is a figure for the magnitude of the electrojet used almost universally in estimating and studying geomagnetic effects, including in Kappernam and Albertson, 1990.

7.3.2 Frequency

The rate of change of the electrojet is also an extremely important factor contributing to the magnitude of induced network currents. In this thesis the electrojet model varies sinusoidally. A period of two minutes, corresponding to a frequency of 0.0083333 Hz, was used as a reasonable estimate of the average rate of change for electrojet currents during a geomagnetic storm (Daglis, 1997).

7.3.3 Height

The effect that the height has on the current induced in the network depends on the location and orientation of the network below the electrojet. A realistic height of 100 km was used. This height corresponds to a layer of the ionosphere where current can flow perpendicular to magnetic lines of flux, a condition required for sustaining the electrojet (Richmond, 1996).

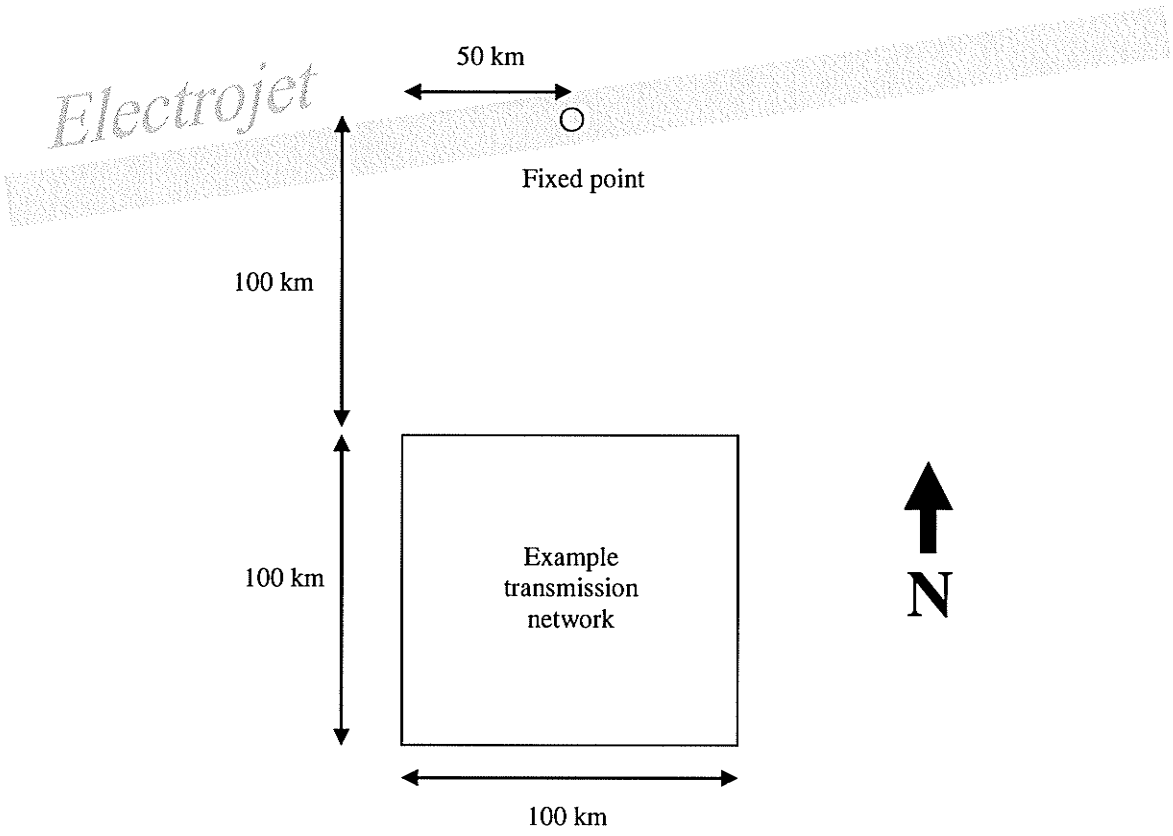

Figure 7.1 Location of electrojet relative to transmission line network

7.3.4 Position

The geographic location of the electrojet is defined by a fixed point and an orientation. For the demonstration in this thesis the fixed point is located 100 km north of the northern-most transmission line in the network. In the east-west or x direction the fixed point is located in the centre of the northern-most transmission line. This puts it exactly between the north-south oriented lines. Figure 7.1 shows the location of the centre point relative to the transmission line network.

The location 100 km north of the transmission network was chosen to help show the effect of the non-uniform field when the electrojet is oriented in the east-west direction. Figure 7.2 shows the general shape of the magnitude of the electric field under an infinite line current. The difference in electric field between locations 100 km from the center and 200 km from the centre is significant and forms to a steep portion of the curve. This difference, which corresponds to the distances of the east-west directed transmission lines under the electrojet when the electrojet is oriented in parallel with them, will highlight the differences between the in-line and the grounded voltage sources.

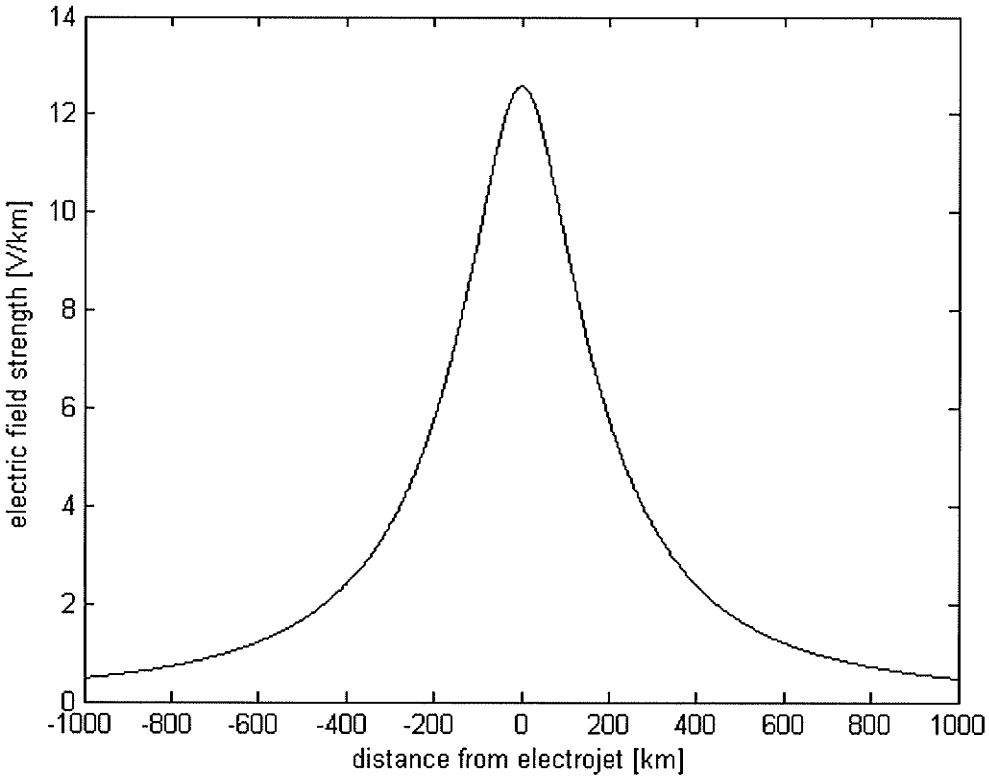

Figure 7.2 Magnitude of the parallel electric field under a typical electrojet

Locating the centre of the electrojet exactly between the north-south directed transmission lines means that when the electrojet is oriented north-south the transmission network is exposed to a balanced electric field. With transmission lines in this particular layout, such a balanced field is effectively a uniform field. This effective uniform field should be correctly represented by both in-line and grounded voltage sources and allows for a check to ensure that differences in results occur only where they are expected.

7.3.5 Ground model

Because the example transmission lines are located in southern Manitoba, the "southern" ground model was used. This choice is a matter of convenience only. The difference between in-line and grounded voltage sources would be apparent regardless of the choice of ground model. While it will influence the shape of the electric field and therefore the exact behaviour of the network, this effect is not what is being studied in this thesis and would not significantly affect the results.

7.3.6 Orientation

To demonstrate the difference between the two models for a variety of configurations the orientation of the electrojet was varied in 15 degree increments from 0 degrees (north directed) to 180 degrees (south directed).

7.4 Transmission Lines

For the sake of simplicity and to show that grounded voltage sources actually do produce erroneous results even on the simplest of networks, 4 perfectly straight transmission lines were used. They form a square 100 km on each side. Since the Earth's surface is modeled as a plane the north-south directed lines are perfectly orthogonal to the east-west lines. The coordinates of the square formed by the transmission lines are not important to the results, but the locations used in this thesis place it in southern Manitoba, enclosing Portage La Prairie and reaching close to the U.S. border. These transmission lines are fictional; they do not actually exist and are used in this thesis for the sake of simplicity. A location within Manitoba was chosen because the induced voltage calculation routine was written with typical Manitoba ground resistivities and checks that transmission lines are approximately inside the Province. Table 7.2 shows the beginning and end points of the 4 transmission lines in UTM coordinates. All coordinates are UTM zone 14 N.

Line name	Start point		End point	
	x	y	x	y
T-Line1	506377	5444491	506377	5544491
T-Line2	506377	5544491	606377	5544491
T-Line3	606377	5544491	606377	5444491
T-Line4	606377	5444491	506377	5444491

Table 7.2 Transmission line coordinates

7.5 Network Conditions Beneath Uniform Electric Field

Tables 7.3 – 7.6 show the predicted currents at the 4 transmission stations for models using in-line and grounded voltage sources under a uniform electric field at a variety of orientations.

Electric field heading [degrees from true north]	Station A current into the ground [A] in-line sources	grounded sources
0	-99.45650362	-99.45650362
15	-121.8088427	-121.8088427
30	-135.8601105	-135.8601105
45	-140.6527363	-140.6527363
60	-135.8601105	-135.8601105
75	-121.8088427	-121.8088427
90	-99.45650362	-99.45650362
105	-70.32636815	-70.32636815
120	-36.40360690	-36.40360690
135	-.1250504762E-11	-.1210485705E-11
150	36.40360690	36.40360690
165	70.32636815	70.32636815
180	99.45650362	99.45650362

Table 7.3 Comparison of station A ground current under uniform electric field

Electric field heading [degrees from true north]	Station B current into the ground [A] in-line sources	grounded sources
0	99.45650362	99.45650362
15	70.32636815	70.32636815
30	36.40360690	36.40360690
45	-.1250505180E-11	-.1264766070E-11
60	-36.40360690	-36.40360690
75	-70.32636815	-70.32636815
90	-99.45650362	-99.45650362
105	-121.8088427	-121.8088427
120	-135.8601105	-135.8601105
135	-140.6527363	-140.6527363
150	-135.8601105	-135.8601105
165	-121.8088427	-121.8088427
180	-99.45650362	-99.45650362

Table 7.4 Comparison of station B ground current under uniform electric field

Electric field heading [degrees from true north]	Station C current into the ground [A] in-line sources	grounded sources
0	99.45650362	99.45650362
15	121.8088427	121.8088427
30	135.8601105	135.8601105
45	140.6527363	140.6527363
60	135.8601105	135.8601105
75	121.8088427	121.8088427
90	99.45650362	99.45650362
105	70.32636815	70.32636815
120	36.40360690	36.40360690
135	0.1250505180E-11	0.1319046435E-11
150	-36.40360690	-36.40360690
165	-70.32636815	-70.32636815
180	-99.45650362	-99.45650362

Table 7.5 Comparison of station C ground current under uniform electric field

Electric field heading [degrees from true north]	Station D current into the ground [A] in-line sources	grounded sources
0	-99.45650362	-99.45650362
15	-70.32636815	-70.32636815
30	-36.40360690	-36.40360690
45	0.1250504849E-11	0.1235990477E-11
60	36.40360690	36.40360690
75	70.32636815	70.32636815
90	99.45650362	99.45650362
105	121.8088427	121.8088427
120	135.8601105	135.8601105
135	140.6527363	140.6527363
150	135.8601105	135.8601105
165	121.8088427	121.8088427
180	99.45650362	99.45650362

Table 7.6 Comparison of station D ground current under uniform electric field

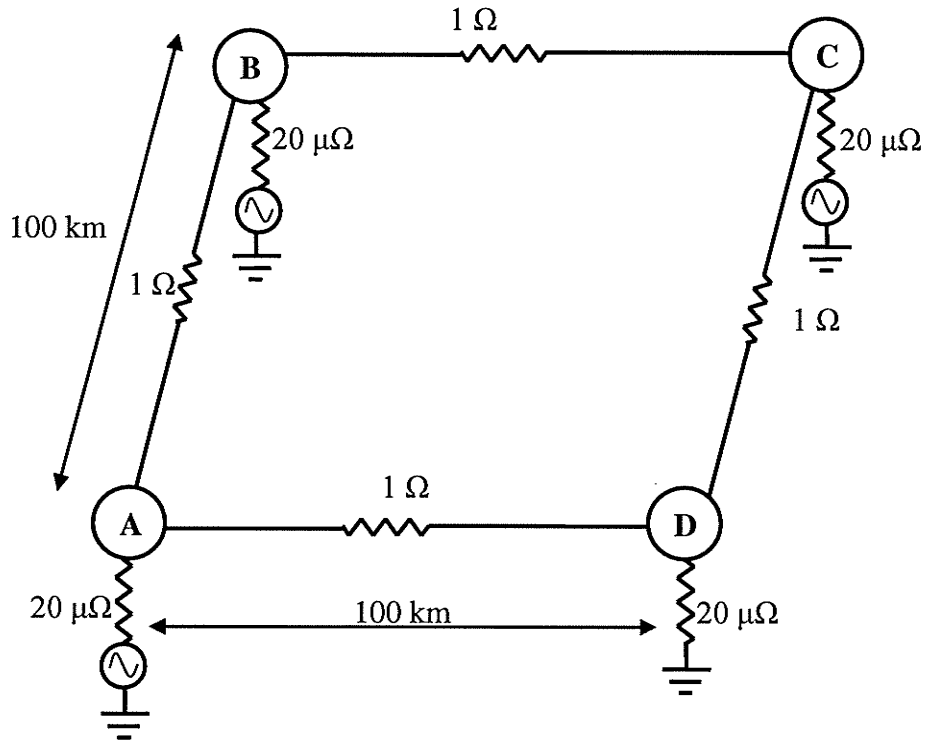

Figure 7.3 Illustration of the demonstration network with grounded voltage sources

The results above agree with the expected outcome that the results should be the same. Even when displaying 10 significant digits, the difference between the models can only be seen where zero current would be expected and the computer simulation produces an extremely small non-zero result. These results (for example the results for 45 degrees in Table 7.6) are, for all practical purposes, zero but are included in detail to show that the computer models did provide slightly different results. These slightly different results confirm that the two models were using different methods to produce the exact same results in the other cases.

7.6 Network Conditions Beneath Realistic Electric Field

Tables 7.7 – 7.10 show the results from the simulation of a non-uniform electric field under the simple transmission networks described above.

Electrojet heading [degrees from true north]	Station A current into the ground [kA] in-line sources	grounded sources
0	1.146933062	1.146933062
15	1.492991353	1.475516159
30	1.507264684	1.409218225
45	1.293730011	1.088103411
60	1.026438075	0.733054702
75	0.781808344	0.435741508
90	0.57277112	0.209503104
105	0.388126018	4.21E-02
120	0.207027337	-8.64E-02
135	1.31E-14	-0.2056266
150	-0.275447071	-0.37349353
165	-0.667406198	-0.684881393
180	-1.146933062	-1.146933062

Table 7.7 Comparison of station A ground current under realistic electric field

Electrojet heading [degrees from true north]	Station B current into the ground [kA] in-line sources	grounded sources
0	-1.146933062	-1.146933062
15	-0.893261699	-1.119121716
30	-0.471524331	-0.667605513
45	2.11E-14	2.99E-14
60	0.40261104	0.598198654
75	0.709339488	1.030559382
90	0.936031871	1.299299888
105	1.103021813	1.424241707
120	1.222021778	1.417609393
135	1.293730011	1.293730011
150	1.311187424	1.115106242
165	1.267135853	1.041275835
180	1.146933062	1.146933062

Table 7.8 Comparison of station B ground current under realistic electric field

Electrojet heading [degrees from true north]	Station C current into the ground [kA] in-line sources	grounded sources
0	-1.146933062	-1.146933062
15	-1.267135853	-1.023805158
30	-1.311187424	-1.017063705
45	-1.293730011	-1.088103411
60	-1.222021778	-1.124222107
75	-1.103021813	-1.078168448
90	-0.936031871	-0.936024606
105	-0.709339488	-0.684486123
120	-0.40261104	-0.304811369
135	-2.44E-14	0.2056266
150	0.471524331	0.76564805
165	0.893261699	1.136592394
180	1.146933062	1.146933062

Table 7.9 Comparison of station C ground current under realistic electric field

Electrojet heading [degrees from true north]	Station D current into the ground [kA] in-line sources	grounded sources
0	1.146933062	1.146933062
15	0.667406198	0.667410715
30	0.275447071	0.275450992
45	-1.25E-14	-1.25E-14
60	-0.207027337	-0.207031249
75	-0.388126018	-0.388132442
90	-0.57277112	-0.572778385
105	-0.781808344	-0.781814768
120	-1.026438075	-1.026441987
135	-1.293730011	-1.293730011
150	-1.507264684	-1.507260762
165	-1.492991353	-1.492986836
180	-1.146933062	-1.146933062

Table 7.10 Comparison of station D ground current under realistic electric field

As predicted, the two models report the same results when the electrojet is oriented at 0 or 180 degrees. At these angles the A-B and C-D transmission lines would have the same voltage induced on them and the B-C and the D-A transmission lines would have no voltage induced on them. The field would therefore appear uniform and the two models should report the same results.

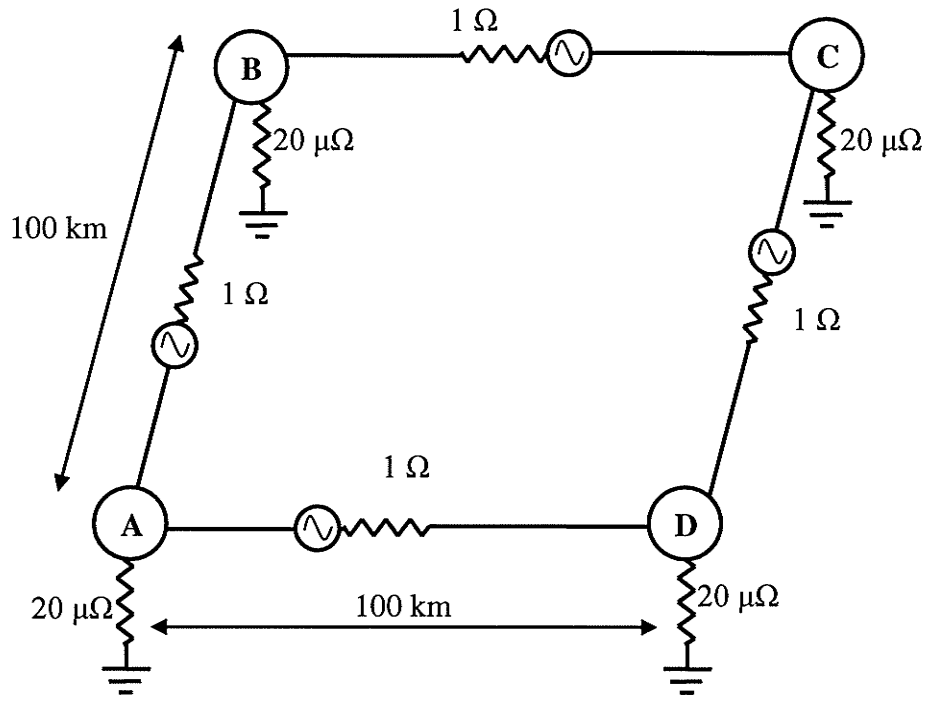

Figure 7.4 Illustration of the demonstration network with in-line voltage sources

The results also clearly show the two models producing different results under most orientations. The in-line voltage sources produce results that are clearly more realistic. Table 7.11 shows a comparison of the results when the electrojet is oriented at 90 degrees east of north. At this angle the only measurable current flowing should be from C to B and from D to A, as there would be no north-south directed electric field component. The table shows that the in-line model produces currents flowing out of station D into station A, and out of station C into station B, as predicted. The grounded model shows very similar currents flowing out of stations C and D, but they do not match the currents

flowing back into the ground at stations B and A. Because of the realistic, non-uniform electric field, the grounded source at station B draws current from both stations C and , incorrectly, from station A. The grounded voltage source model has substantial currents flowing between nodes A and B where ideally there would be none and in this model there should be vanishingly little. Table 7.11 shows that the grounded voltage source model cannot be used on simulations using realistic electrojet models.

	Current into the ground at station [kA]			
Model	A	B	C	D
in-line	0.57277112	0.936031871	-0.936031871	-0.57277112
grounded	0.209503104	1.299299888	-0.936024606	-0.572778385

Table 7.11 Comparison of ground currents under a simulated electrojet oriented 90 degrees east of north.

If the station grounding resistances were larger a potential difference would have appeared between nodes A and B and nodes C and D and a current would have flowed perpendicular to the electric field. This effect is not the same as the spurious potential difference that appears when using grounded voltage sources, which is explained in section 4.3.1 of chapter 4, but is caused by finite station ground resistances. It is not a weakness of the model, but the realistic result of a network with finite ground resistances. Because the station ground resistances were purposely made very small in the cases used, the potential difference between nodes A and B and nodes C and D are negligibly small.

7.7 Conclusion

By using the Multi-Run component in PSCAD the effects of 13 different orientations of realistic and uniform electric fields were modeled on 2 transmission network models. As predicted, the results show that grounded voltage sources are unable to model the effects of non-uniform electric field in networks. Power system simulations involving realistic electrojet models, like those required to accurately model Manitoba, require the use of in-line voltage sources.

Chapter 8

Conclusion

8.1 Thesis Summary

This thesis dealt with the modeling of Geomagnetically Induced Currents (GICs) on networked conductors. The cause of Geomagnetically Induced Currents is the auroral electrojet, a high altitude electric current. The processes that create and influence this current were introduced and explained. The effects that the electrojet causes near the surface of the Earth were investigated. It was concluded that, for studies at high latitudes, a non-uniform influence near the surface must be modeled. An appropriate approximation of the electrojet was chosen and two methods of calculating the electric field created by this electrojet were compared. The complex-image calculation method was chosen and used in this thesis. Weaknesses of the accepted Earth-surface-potential explanation for GICs were discussed. Theoretical examples were used to show the necessity of using in-line voltage sources when modeling the effects of non-uniform fields. A method for calculating the total voltage induced along the path of an arbitrary conductor, given electrojet parameters and the path of a conductor, was described. Finally, a power system simulator, PSCAD, was used to compare networks modeled with grounded sources and in-line voltage sources. The results confirmed that in-line voltage sources are required to correctly model realistic GIC flow in networks.

8.2 Main Contributions

Models of an electrojet, a multi-layer earth, the resultant electric field, transmission line paths, and an electrical network were combined into a single simulation. The need to know the in-line voltage induced on a line created a situation unusual in power system studies. The geographic characteristics of a transmission line are needed to calculate an electrical characteristic. A routine was created to combine geographic information about a transmission line with geographic and electrical characteristics of an auroral electrojet and produce an electrical value induced on the given transmission line as output. This induced voltage calculation routine was successfully incorporated into PSCAD, which will allow the simulation of more complicated models.

The characteristics of the electrojet can be modified within the PSCAD graphical user interface and the output of the routine is used to control in-line voltage sources in a network model. PSCAD is used to calculate the geomagnetically induced currents (GICs) in the electrical network for a given set of transmission lines and electrojet parameters.

8.3 Further Developments

Incorporating the electrojet and transmission line routes into PSCAD, a power system simulator, allows for significant future developments. Realistic AC power systems could be modeled with the influence of GIC. With the use of an accurate transformer model, the effects of a given electrojet on the reactive power consumption of a power system could be modeled (Chandrasena et al., 2004). Theoretically, with sufficiently detailed modeling of the power system, one could determine the magnitude of electrojet required to cause voltage collapse in a given system.

There are also possibilities for further development of the voltage calculation routine. A current filament is obviously only an approximation to the auroral electrojet. Because superposition holds, multiple filaments could be used to represent an electrojet with finite width. The Frequency of the electrojet is a very important parameter which could be developed further. Multiple frequencies could be modeled simultaneously with multiple voltage sources. One can imagine that Fourier transforms could be used to model the electrojet that produced a particular recorded GIC at a specific location. This electrojet model could then be used to approximate the GIC at other locations at the time when the recording was made.

References

Akasofu, S., 1968. *Polar and Magnetospheric Substorms*, Springer-Verlag, New York, 280pp.

Akasofu, Syun-Ichi, 1992. Aurora, in: Suess, Steven T., Tsurutani, Bruce T. [Eds], 1998. *From the Sun: Auroras, Magnetic Storms, Solar Flares, Cosmic Rays*, American Geophysical Union, Washington, 172pp.

Albertson, Vernon D., Van Baelen, Johan A., 1970, Electric and magnetic fields at the Earth's surface due to auroral currents, *IEEE transactions on power apparatus and systems*, Vol. PAS-80, No. 4, April 1970, pp 578-584.

Albertson, Vernon D., Thorson, J.M. Jr., Miske, S.A. Jr., 1974, the effects of geomagnetic storms on electrical power systems, *IEEE transactions on power apparatus and systems*, Vol. PAS-93, No. 4, July/August 1974, pp 1031-1044.

Albertson, Vernon D., Kappenman, J.G., Mohan, N., Skarbakka, G.A., 1981, load-flow studies in the presence of geomagnetically-induced currents, *IEEE transactions on power apparatus and systems*, Vol. PAS-100, No.2, February 1981, pp 594- 607.

Autodesk, 1997, AutoCAD release 14 user's guide, catalogue number 00114-000000-5010, March 29, 1997.

Bolduc, Léonard., Granger, Michel., Paré, Grégoire., Sintonge, Jean., Brophy, Luc., 2005, Development of a DC Current-Blocking Devince for Transformer Neutrals, *IEEE transactions on power delivery*, Vol. 20, No. 1, January 2005, pp 163-168.

Boteler, D.H., 1994, Geomagnetically Induced Currents: present knowledge and future research, *IEEE transactions on power delivery*, Vol. 9, No. 1, January 1994, pp 50-58.

Boteler, D.H., Bui-Van, Q., Lemay, J., 1994, directional sensitivity to geomagnetically induced currents of the Hydro-Quebéc 735 kV power system, *IEEE transactions on power delivery*, Vol. 9, No. 4, October 1994, pp 1963-1971.

Boteler, D.H., Pirjola, R.J., 1998a, The complex-image method for calculating the magnetic and electric fields produced at the surface of the Earth by the auroral electrojet, *Geophysical Journal International*, 132, pp 31-40.

Boteler, D.H., Pirjola, R.J., 1998b, modeling geomagnetically induced currents produced by realistic and uniform electric fields, *IEEE transactions on power delivery*, Vol. 13, No. 4, October 1998, pp 1303-1308.

Boteler, D.H., Watanabe, T., Shier, R.M., Horita, R.E., 1982, characteristics of geomagnetically induced currents in the B.C. Hydro 500 kV system, *IEEE transactions on power apparatus and systems*, Vol. PAS-101, No. 6, June 1982, pp 1447-1456.

Campbell, Wallace H., 1997. *Introduction to Geomagnetic Fields*, Cambridge University Press, Cambridge, 290pp.

Chandrasena, W., McLaren, P.G., Annakkage, U.D., Jayasinghe, R.P., An Improved Low-Frequency Transformer Model for Use in GIC Studies, *IEEE Transactions on Power Delivery*, Vol. 19, No. 2, April 2004, pp 643-651.

Cheng, David, K., 1989. *Field and Wave Electromagnetics – Second Edition*, Addison-Wesley, Don Mills, Ontario, 703pp.

Cowley, S.W.H., 1995. The Earth's Magnetosphere, in: Suess, Steven T., Tsurutani, Bruce T. [Eds], 1998. *From the Sun: Auroras, Magnetic Storms, Solar Flares, Cosmic Rays*, American Geophysical Union, Washington, 172pp.

Dana, Peter H., 1999. Coordinate Systems Overview [online], Accessed October 6 2005, Available: http://www.colorado.edu/geography/gcraft/notes/coordsys/coordsys_f.html.

Daglis, Ioannis A., 1997. The Role of Magnetospheric-Ionospheric Coupling in Magnetic Storm Dynamics, in: Tsurutani, Bruce T., et all.[Eds], 1997. *Magnetic Storms*, Geophysical Monograph 98, American Geophysical Union, Washington, 266pp.

EPRI Power System Dynamics Tutorial, EPRI, Palo Alto, CA: 2002. 1001983.

Farrugia, C.J., et al., 1997. Magnetic Coulds and the Quiet-Storm Effect at Earth, in: Tsurutani, Bruce T., et all.[Eds], 1997. *Magnetic Storms*, Geophysical Monograph 98, American Geophysical Union, Washington, 266pp.

Gallant, Roy A., 1980. *National Geographic Picture Atlas of Our Universe*, National Geographic Society, Washington, 276pp.

Goldstein, B.E., 1993. The Solar Wind, in: Suess, Steven T., Tsurutani, Bruce T. [Eds], 1998. *From the Sun: Auroras, Magnetic Storms, Solar Flares, Cosmic Rays*, American Geophysical Union, Washington, 172pp.

Gonzalez, W.D., et al., 1994. *What is a Geomagnetic Storm?*, J.Geophys., Res. 99, 5771.

Hermance, J.F., Peltier, W.R., 1970, magnetotelluric fields of a line current, *Journal of Geophysical Research*, 75, 3351-3356.

IEEE Working Group, B. Bozoki, Chairman: The Effects of GIC on Protective Relaying, *IEEE Transactions on Power Delivery*, Vol. 11, No. 2, April 1996, pp 725-739

Jackson, Bernard V., 1997. Heliospheric Observations of Solar Disturbances and Their Potential Role in the Origin of Geomagnetic Storms, in: Tsurutani, Bruce T., et all.[Eds], 1997. *Magnetic Storms*, Geophysical Monograph 98, American Geophysical Union, Washington, 266pp.

Jayasinghe, R.P., McLaren, P.G., Goldsborough, T., 1993, Effect of GIC on Overcurrent Protection for Filter Banks, in Proc. WESCANEX 93 'Communications, Computers and Power in the Modern Environment', Saskatoon, May 1993, pp 36-42

Kappenman, John G., Alberson, Vernon D., 1990, Bracing for the geomagnetic storms, IEEE Spectrum, March 1990, pp 27-33.

Manitoba HVDC Research Centre Inc., 2004, PSCAD Version 4.0 On-Line Help System, [electronic].

Manitoba Hydro, 1977, Specification No.1501 – Dorsey Station 500 kV System – Supply of Single Phase Auto-Transformers, Invitation to Tender, May 1977.

McPherron, R.L., 1997. The Role of Substorms in the Generation of Magnetic Storms, in: Tsurutani, Bruce T., et all.[Eds], 1997. *Magnetic Storms*, Geophysical Monograph 98, American Geophysical Union, Washington, 266pp.

Parkinson, W.D., 1986. *Introduction to Geomagnetism*, Elsevier, New York, 433pp.

Pirjola, Risto., 1996, GIC Seminar [Seminar Notes], Seminar Given to Manitoba Hydro, May 13-14, Winnipeg.

Pirjola, Risto., 2002, Review of the calculation of surface electric and magnetic fields and geomagnetically induced currents in ground-based technological systems, *Surveys in Geophysics*, vol. 23, no. 1, pp 71-90.

Pirjola, Risto J., 1998, modeling the electric and magnetic fields at the Earth's surface due to an auroral electrojet, *Journal of atmospheric and solar-terrestrial physics*, no. 60, pp 1139-1148.

Pirjola, R., Viljanen, A., 1989, on geomagnetically-induced currents in the Finnish 400kV power system by an auroral electrojet current, *IEEE Transactions on Power Delivery*, Vol. 4, No. 2, April 1989, pp 1239-1245.

Prabhakara, F.S., Hannett, L.N., Ringlee, R.J., Ponder, J.Z., 1992, geomagnetic effects modeling for the PJM interconnection system part II – geomagnetically induced current study results, *IEEE transactions on power systems*, Vol. 7, No. 2, May 1992, pp 565-571.

Price, Philip R., 2002, geomagnetically induced current effects on transformers, *IEEE transactions on power delivery*, Vol. 17, No. 4, October 2002, pp 1002-1008.

Richmond, A.D., 1996. The Ionosphere and Upper Atmosphere, in: Suess, Steven T., Tsurutani, Bruce T. [Eds], 1998. *From the Sun: Auroras, Magnetic Storms, Solar Flares, Cosmic Rays*, American Geophysical Union, Washington, 172pp.

Sadiku, M.N.O., 1994, *Elements of Electromagnetics second edition*, Saunders College Publishing, Toronto, 1994.

Suess, Steven T., Tsurutani, Bruce T. [Eds], 1998. *From the Sun: Auroras, Magnetic Storms, Solar Flares, Cosmic Rays*, American Geophysical Union, Washington, 172pp.

Swatek, David R., 2000, "Surface Impedance of Layered Earth Illuminated by Vertically directred Plane Waves", unpublished.

Tay, Hock-Chuan., Swift, Glen W., On the Problem of Transformer Overheating Due to Geomagnetically Induced Currents, *IEEE transactions on power apparatus and systems*, Vol. PAS-104, No. 1, January 1985, pp 212-219.

Towle, J.N, Prabhakara, F.S., Ponder, J.Z., 1992, geomagnetic effects modeling for the PJM interconnection system part I – Earth surface potentials computation, *IEEE transactions on power systems*, Vol. 7, No. 3, August 1992, pp 949-955.

Tsurutani, Bruce T., Gonzalez, Walter D., 1994. Magnetic Storms, in: Suess, Steven T., Tsurutani, Bruce T. [Eds], 1998. *From the Sun: Auroras, Magnetic Storms, Solar Flares, Cosmic Rays*, American Geophysical Union, Washington, 172pp.

Tsurutani, Bruce T., Gonzalez, Walter D., 1997. The Interplanetary Causes of Magnetic Storms: A Review, in: Tsurutani, Bruce T., et all.[Eds], 1997. *Magnetic Storms*, Geophysical Monograph 98, American Geophysical Union, Washington, 266pp.

Van Allen, James A., 1991, Radiation Belts, in: Suess, Steven T., Tsurutani, Bruce T. [Eds], 1998. *From the Sun: Auroras, Magnetic Storms, Solar Flares, Cosmic Rays*, American Geophysical Union, Washington, 172pp.

Wait, J.R., Spies, K.P., 1969, on the representation of the quasi-static fields of a line current source above the ground, *Canadian Journal of Physics*, 47, pp 2731-2733.

Appendix A

A.1 Layered earth ground models from Pirjola (1996)

Layer Number	Thickness (h) [m]	Resistivity (ρ) [Ωm]
1	20	20
2	180	100
3	14 800	40 000
4	10 000	2000
5	15 000	1000
6	60 000	1000
7	300 000	100
8	200 000	10
9	-	1

Table A.12 Southern Manitoba ground model

Layer Number	Thickness (h) [m]	Resistivity (ρ) [Ωm]
1	10	20
2	150	100
3	14 740	20 000
4	10 000	1000
5	15 000	500
6	60 000	500
7	300 000	100
8	200 000	10
9	-	1

Table A.13 Northern Manitoba ground model

A.2 Reflection coefficient equations from Hermance & Peltier (1970)

$$R = \frac{(\theta_1 - \lambda) + (\theta_1 + \lambda)R'e^{-2\theta_1 d}}{(\theta_1 + \lambda) + (\theta_1 - \lambda)R'e^{-2\theta_1 d}} \quad \text{(A-1)}$$

where;

$$R' = \frac{\theta_2 - \theta_1}{\theta_2 + \theta_1}, \quad \text{(A-2)}$$

$$\theta_j = \lambda^2 + i\omega\mu\sigma_j \quad \text{(A-3)}$$

and

σ_j is the earth conductivity at the jth layer.

A.3 Surface impedance calculation from Swatek (2000)

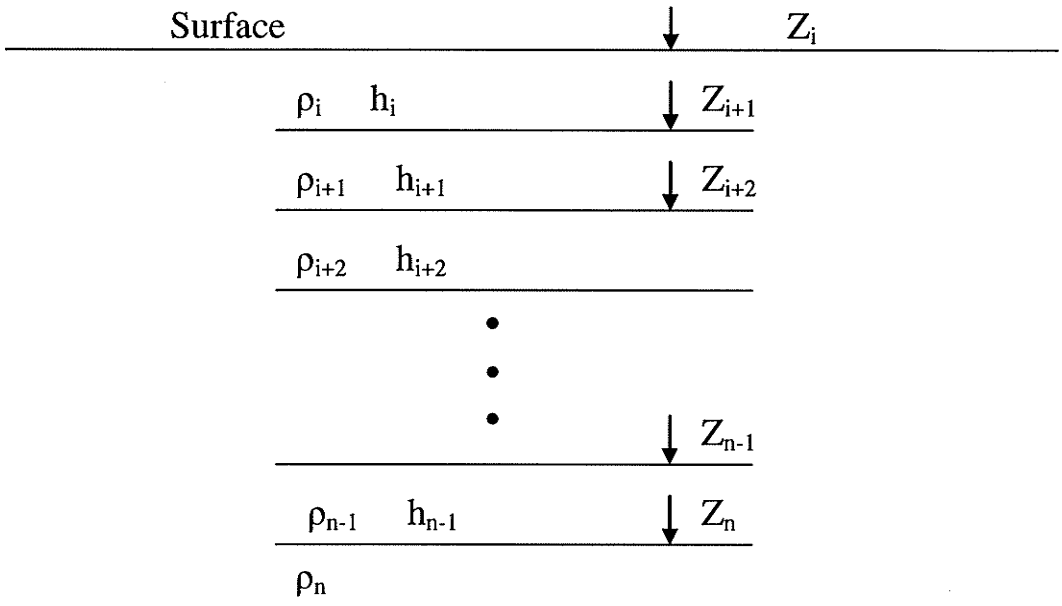

Figure A.1 Layered earth model.

The impedance of the deepest (*n*th) layer of earth is given by:

$$Z_n = \sqrt{\omega \mu_n \rho_n} \cdot e^{j\pi/4} \qquad \text{(A-4)}$$

Where ρ_n is the ground resistivity in Ω meters of the n^{th} layer and μ_n is the permeability of the n^{th} layer.

The reflection coefficient looking into the $i+1^{th}$ layer (where the i^{th} layer is the one above) is given by:

$$\Gamma_{i+1} = \frac{Z_{i+1} - \frac{\omega\mu_i}{k_i}}{Z_{i+1} + \frac{\omega\mu_i}{k_i}} \qquad \text{(A-5)}$$

Where k_i is the wave number of the i^{th} layer, found using:

$$k_i = \sqrt{\omega^2\varepsilon_i\mu_i - \frac{j\omega\mu_i}{\rho_i}}, \qquad \text{(A-6)}$$

Where ε_i is the permittivity of the i^{th} layer. If $\omega\varepsilon_i << 1/\rho_i$ this can be approximated as:

$$k_i \approx \sqrt{\frac{\omega\mu_i}{\rho_i}} \cdot e^{-j\frac{\pi}{4}} \qquad \text{(A-7)}$$

From the above, the impedance looking into the i^{th} layer can be found using:

$$Z_i = \frac{\mu_i\omega}{k_i} \cdot \left(\frac{1 + \Gamma_{i+1}e^{-2jk_ih_i}}{1 + \Gamma_{i+1}e^{-2jk_ih_i}} \right) \qquad \text{(A-8)}$$

Where h_i is the depth of the i^{th} layer. This method can be repeated as often as required to find the surface impedance using an arbitrary number of layers.

Appendix B

B.1 Derivation of the equation for the distance from points directly under the electrojet

The electrojet is defined by a fixed point, (cx,cy) and an angle. For this derivation the angle (γ) will be measured between the x-axis and the axis of the electrojet.

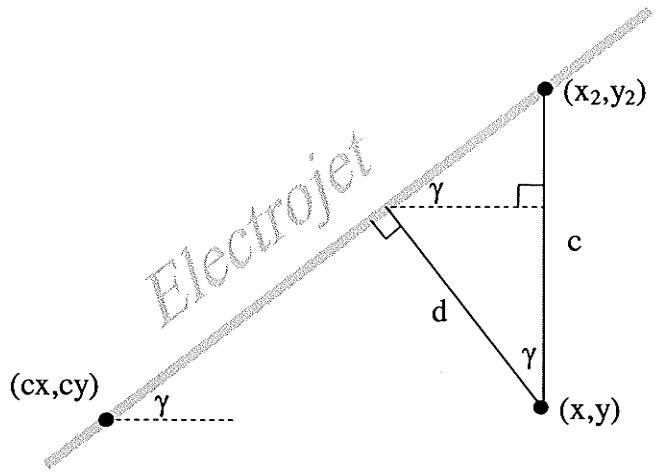

Figure B.1 Diagram of point-electrojet distance

In order to measure the perpendicular distance between a point directly under the electrojet and an arbitrary point a simple and robust formula was required. From Figure B.1 it can be seen that:

$$Cos(\gamma) = d/c \tag{B-1}$$

Since,

$$c = y_2 - y \tag{B-2}$$

and from the definition of slope,

$$y_2 = cy + m\,(x\text{-}cx) \tag{B-3}$$

which, for the general case, yields:

$$d = \left|\cos(\gamma)\{[cy + \tan(\gamma)\,(x - cx)] - y\}\right| \tag{B-4}$$

Which can be used to find the minimum distance between a line defined by a fixed point and a heading and any arbitrary point.

B.2 Flat-Earth vs. great-circle distance calculations:

Taking 2 points at opposite corners of Manitoba,

49.0 N 96.0 W

and

60.0 N 101 W

the distance between the points assuming a spherical Earth can be calculated by:

$$D = R_e \cdot \arccos(\cos(lon1 - lon2) \cdot \cos(lat1) \cdot \cos(lat2) + \sin(lat1) \cdot \sin(lat2)$$

Where R_e is the radius of the Earth, approximately 6371000 m this gives a distance of:

$D = 1.264 \times 10^6\ m$

Using any conversion tool, these lat-long coordinates can be converted to UTM.

49.0 N 96.0 W becomes:

Easting: 719413.7014754937 Northing: 5431793.0146558955

and 60.0 N 101 W becomes:

Easting: 388455.9605090685 Northing: 6653097.61958313

Assuming a flat-Earth and calculating the distance between these points using Pythagoras yields:

$D = 1.265 \times 10^6$ m.

An error of 1 km over the whole province is more than acceptable considering the other approximations used in physical parametrs.

Appendix C

C.1 Subroutine Vin.f

```
      Subroutine Vin(n,i,f,h,cx,cy,deg,north,filenm,Esum)


      include 'emtstor.h'
      include 'emtconst.h'
      include 'nd.h'
      include 's1.h'


      integer num, errornum,k,n, count, north
      character*50 char,filenm
      real    h, I, ro(9), ht(9)
      real(8) l, dx, dy, E, Eavg, Esum, Eprev,x,y,cx,cy,xprev,yprev,ang&
     &  ,deg, angr, m, f, d, u, w, pr, pi, angd, Erms
      logical error
      complex(8) j,p, Ec, Ki, R, z
!*****************************************************************
      error = .false.
      xprev=0
      yprev=0
      x=0
      y=0
```

```
        E=0
        Eprev=0
        num = 0
        Esum=0
        Erms=0
        d=0
        R=0
        z=0
        u=PI_*4E-7
        w=f*TWO_PI
!       finds angular frequency
        j=(0,1)
!***********************************************

        if (north.EQ.0) then

        ro(1)=20
        ro(2)=100
        ro(3)=40000
        ro(4)=2000
        ro(5)=1000
        ro(6)=1000
        ro(7)=100
```

```
ro(8)=10

ro(9)=1


ht(1)=20

ht(2)=180

ht(3)=14800

ht(4)=10000

ht(5)=15000

ht(6)=60000

ht(7)=300000

ht(8)=200000

ht(9)=0


else if (north.EQ.1) then


ro(1)=20

ro(2)=100

ro(3)=20000

ro(4)=1000

ro(5)=500

ro(6)=500

ro(7)=100

ro(8)=10
```

```
      ro(9)=1


      ht(1)=10

      ht(2)=250

      ht(3)=14740

      ht(4)=10000

      ht(5)=15000

      ht(6)=60000

      ht(7)=300000

      ht(8)=200000

      ht(9)=0


      endif


      z=sqrt((w*u)*ro(9))*exp(j*(PI_/4))


      count = 8

      do while (count.GE.1)

      Ki=sqrt(w*u*(1/ro(count)))*exp(-j*(PI_/4))

      R=((z-((w*u)/Ki))/(z+((w*u)/Ki)))

      z=((w*u)/Ki)*((1+R*exp(-2*j*Ki*ht(count)))/(1-R*exp(-2*j*Ki*&
&ht(count))))

      count = count-1
```

```
        end do



        p=(z/(j*w*u))
        print*, 'P=', p
!*****************************************************************
        angd= 90-deg
!       converts from zero at north to zero along X axis.
        angr=angd*(PI_BY180)
!       convert degrees to rads
        m= TAN(angr)
!       finds slope


        open (unit=90,file=filenm,status='old')
!*****************************************************************
50      read (90,*) char
        num=num+1
        do while (char.NE.'ENTITIES'.AND.char.NE.'EOF')
        read (90,*) char
        num=num+1
        end do
!       searches for ENTITIES section
```

```
                do while (char.NE.'ENDSEC'.AND.char.NE.'EOF')
!               avoids reading past the last entry
                read (90,*) char
                num=num+1

                    if (char.EQ.'10')then
                    read (90,*) x, char, y
                    num=num+3

!                       The X co-ordinate is preceded by a 10 and followed by a 20
which in turn precedes the Y
                        if
(x.LT.160000.OR.x.GT.1000000.OR.y.LT.4446000.OR.y.&
   &                    GT.7228000) then
!                       These are the maximum and minumum permisible values
for UTM co-ordinates
                        error = .true.
                        errornum = num
                        go to 100
                        end if

                        if (xprev.EQ.0) then
```

```
                    go to 70
                    end if
!                   ensures no calculations are done untill there is a line section
(no calc done on first data point)
!*********************************************************************
                    if ((x-xprev).NE.0) then
                    ang = ATAN((y-yprev)/(x-xprev))
                    else
                    ang = PI_BY2
                    end if

                    dx=((x-xprev)/n)
                    dy=((y-yprev)/n)
                    l=sqrt((dx**2)+(dy**2))

                    E=0

                    do 60 k=0,n
                    x=xprev+k*dx
                    y=yprev+k*dy

                        if (angd.EQ.0.OR.angd.EQ.180) then
```

```
                    d=abs(cy-y)
                    else if (angd.EQ.90.OR.angd.EQ.270) then
                    d=abs(cx-x)
                    else
                    d=abs(cos(angr)*((cy+m*(x-cx))-y))
!                   Calculates the distance to the Electro Jet
                    end if

                    Eprev = E
!*********************************************************************
                    Ec=((w*u*I*j)/(TWO_PI))*log((sqrt(((h+2*p)**2)&
   &                +d**2))/sqrt((h**2)+(d**2)))
                    E=-sqrt((real(Ec)**2)+(aimag(Ec)**2))
!                   E=1
!*********************************************************************

                    if (Eprev.EQ.0) then
                    go to 60
                    end if

                    Eavg=((E+Eprev)/2)

        Esum = Esum + ((dx)*(Eavg*cos(angr)))+((dy)&
```

```
   &*(Eavg*sin(angr)))

60                          continue
!*********************************************************************
70                          xprev=x
                            yprev=y
100                   end if
               end do

               if (.not.error) then
               print*, 'data OK'
               else
               print*, 'Data points that did not conform to UTM co-ordinates'
               print*, 'in or near Manitoba were skiped, they appeared on line'
               print*, errornum
               end if

1000   close (unit=90)
       print*, 'stoped reading at: ',char
!******************
! convert the Esum to RMS, because that's what the sources in PSCAD expect!
       Erms = Esum
       Esum = Esum/SQRT_2
```

```
Print*, 'total rms E field is', Esum, 'i', n, 'steps peak E field is', Erms
end subroutine Vin
```

C.2 FORTRAN script in PSCAD page component

```
IF (TIMEZERO) THEN
print*, 'hello world'
print*, "$filenm"
call Vin($n,$i,$f,$h,$cx,$cy,$ang,$north,"$filenm",$V)
print*, $V, 'volts or', $V/1000, 'kV'
$V = $V/1000
ENDIF
```